Photodiagnosis and Photodynamic Therapy 52 (2025) 104514

Contents lists available at ScienceDirect

Photodiagnosis and Photodynamic Therapy

journal homepage: www.elsevier.com/locate/pdpdt

Research Paper

New insights on antibacterial mode of action of blue-light photoactivated berberine and curcumin-antibiotic combinations against *Staphylococcus aureus*

Ariana S.C. Gonçalves [a,b,c], José R. Fernandes [d,e], Maria José Saavedra [f,g,h,i], Nuno M. Guimarães [a,b], Cristiana Pereira [c,j], Manuel Simões [a,b,k], Anabela Borges [a,b,k,*]

[a] LEPABE-Laboratory for Process Engineering, Environment, Biotechnology and Energy, Faculty of Engineering, University of Porto, Rua Dr. Roberto Frias, s/n, 4200-465, Porto, Portugal
[b] ALICE-Associate Laboratory for Innovation in Chemical Engineering, Faculty of Engineering, University of Porto, Rua Dr. Roberto Frias, s/n, 4200-465, Porto, Portugal
[c] Environmental Health Department, Portuguese National Health Institute Doutor Ricardo Jorge, Porto, Portugal
[d] CQVR-Vila Real Chemistry Center, University of Trás-os-Montes e Alto Douro, Portugal
[e] Physical Department, University of Trás-os-Montes and Alto Douro, Quinta dos Prados, 5000-801, Vila Real, Portugal
[f] Antimicrobials, Biocides and Biofilms Unit (AB2Unit), Laboratory of Medical Microbiology, University of Trás-os-Montes e Alto Douro, 5000-801, Vila Real, Portugal
[g] Animal and Veterinary Research Center (CECAV)-Al4AnimalS, University of Trás-os-Montes e Alto Douro, 5000-801, Vila Real, Portugal
[h] Center Interdisciplinar of Marine and Environmental Research (CIIMAR), University of Porto, 4450-208 Matosinhos, Portugal
[i] Center for the Research and Technology of Agro-Environmental and Biological Sciences (CITAB)-Inov4Agro, University of Trás-os-Montes e Alto Douro, 5000-801 Vila Real, Portugal
[j] Environmental Hygiene and Human Biomonitoring Unit, Department of Health Protection, d, Luxembourg
[k] DEQB-Department of Chemical and Biological Engineering, Faculty of Engineering, University of Porto, Rua Dr. Roberto Frias, s/n, 4200-465 Porto, Portugal

ARTICLE INFO

Keywords:
Antibiotic resistance
Antimicrobial photodynamic inactivation
Berberine/Curcumin-antibiotic combinations
Multi-target
Oxidative stress
S. aureus wound infections
Photodynamic Therapy

ABSTRACT

Antimicrobial photodynamic inactivation (aPDI), using photosensitisers in combination with antibiotics, is a promising multi-target strategy to address antibiotic resistance, particularly in wound infections. This study aimed to elucidate the antibacterial mode of action of combinations of berberine (Ber) or curcumin (Cur) with selected antibiotics (Ber-Ab or Cur-Ab) under blue light irradiation (420 nm) against *Staphylococcus aureus*, including methicillin-resistant (MRSA) and methicillin-susceptible (MSSA) strains. Multiple physiological parameters were assessed using complementary assays (fluorometry, epifluorescence microscopy, flame emission and atomic absorption spectroscopy, zeta potential, flow cytometry, and the plate agar method) to examine the effect on ROS production, membrane integrity, DNA damage, motility and virulence factors of *S. aureus*. Results indicated that blue light photoactivated Ber-Ab and Cur-Ab combinations led to substantial ROS generation, even at low concentrations, causing oxidative stress that severely impacted bacterial membrane integrity (approximately 90 % in MRSA and 40 % in MSSA). Membrane destabilization was further confirmed by elevated intercellular potassium release (≈ 2.00 and 2.40 μg/mL in MRSA and MSSA, respectively). Furthermore, significant DNA damage was observed in both strains (≈ 50 %). aPDI treatment with blue light also reduced *S. aureus* pathogenicity by impairing motility and inhibiting key virulence factors such as proteases, lipases, and gelatinases, all of which play key roles in the infectious process. Overall, Ber-Ab combinations demonstrated the highest efficacy across all parameters tested, highlighting for the first time the multi-target therapeutic potential of this phytochemical-based aPDI strategy to combat antibiotic-resistant *S. aureus* infections and improve wound infection treatment outcomes.

* Corresponding author at: LEPABE-Laboratory for Process Engineering, Environment, Biotechnology and Energy, Faculty of Engineering, University of Porto, Rua Dr. Roberto Frias, s/n, 4200-465, Porto, Portugal.
E-mail address: apborges@fe.up.pt (A. Borges).

https://doi.org/10.1016/j.pdpdt.2025.104514
Received 11 December 2024; Received in revised form 29 January 2025; Accepted 5 February 2025
Available online 6 February 2025

1. Introduction

As the challenges to global healthcare continue to increase, the prevalence of wounds is becoming a critical issue requiring comprehensive strategies for effective management and treatment [1]. Antimicrobial resistance has reached uncontrollable levels, making wound infections a challenge for patients, their families, and healthcare professionals [2]. *Staphylococcus aureus* is indeed one of the most common pathogens infecting wounds, especially the topical ones [3]. Various approaches have been explored to overcome the therapeutic limitations of conventional marketed antibiotics in treating wound infections [4–6]. These include antimicrobial photodynamic inactivation (aPDI) and natural-based antibiotic combinations centered on the premise of multi-targeting effects [4,5]. aPDI is a promising approach to combat antibiotic resistance, especially in topical infections, by harnessing the power of reactive oxygen species (ROS) from the irradiation process [7]. This approach can attack multiple bacterial structures, including cell membranes, functional proteins, and DNA, leading to the death of bacterial pathogens or making them more susceptible to other therapeutic agents, including antibiotics [8]. A crucial aspect of aPDI is that it requires molecular oxygen, light of a specific wavelength, and a non-toxic photosensitiser (PS). The choice of light in aPDI of skin wound infections is crucial, as the health of uninfected cells must be safeguarded [9]. With this in mind, the blue light system has been used as an approach that has low toxicity to cells, depending on irradiance and light doses applied [10]. Regarding PS, several compounds, including methylene and toluidine blue, have shown excellent photodynamic properties [11]. In particular, natural-based PS, such as plant secondary metabolites (phytochemicals), have attracted attention due to their green source [8]. Among the panoply of plant-based PS, curcumin (Cur) is a well-studied phytochemical that has shown remarkable photodynamic abilities in inactivating both Gram-positive and Gram-negative bacteria. Another interesting phytochemical, berberine (Ber), has been explored recently as a PS in aPDI, although its photodynamic properties need to be further investigated [12]. On the other hand, phytochemicals can exhibit remarkable antibacterial activities [13]. Their differentiated/diverse chemical structures can promote the interaction with various bacterial components and help to surpass bacterial resistance mechanisms (*e.g.*, motility, quorum sensing, efflux pumps, extracellular matrix, and others, more detailed information is comprehensively provided in Gonçalves et al. [13]). All these properties make phytochemicals good candidates to restore the effect of less effective antibiotics due to their promising multi-target activity [5]. In particular, Ber and Cur, have also shown the ability to restore the activity of antibiotics by simultaneously interacting with bacterial membranes, DNA, and virulence factors, thereby sensitizing the bacteria to the effects of antibiotics [14,15]. Nonetheless, despite their interesting antibacterial and potentiating activities, Ber and Cur are not used as antimicrobial agents in clinical therapeutic practices.

The dual use of aPDI with natural-based antibiotic combinations has emerged as a potential solution to overcome antibiotic resistance [16]. While the considerable antibacterial activity of ROS is evident, their limited lifetime (3.5 μs) and short diffusion length (≈ 100 nm in an aqueous solution) have been associated with the potential recurrence of infections [17]. For this reason, the synergy of aPDI with phytochemical-antibiotic combinations utilizes the versatile attack of ROS that occurs during photoactivation and the chemotherapeutic properties of antibiotics and phytochemicals, offering a promising strategy to overcome the limitations of both approaches when used individually [18]. However, although recent studies have explored the application of light-activated antibiotic combinations [18], there remains a significant gap in understanding the precise mode of action of aPDI using phytochemical-antibiotic combinations. In particular, to our knowledge, no studies have specifically examined the photoactivation of Ber or Cur combined with clinical topical antibiotics in the context of wound treatment. Additionally, the influence of light on enhancing or altering the antimicrobial action of natural photosensitisers in combination with clinical antibiotics remains to be understood. Therefore, this study fills existing knowledge gaps by investigating for the first time, as far as we know, the mode of action of combinations between Ber or Cur with clinical antibiotics (Ber-Ab or Cur-Ab) under blue light irradiation. A comprehensive understanding of the mode of action of photo- and non-photoactivated Ber-Ab and Cur-Ab combinations could provide new insights into the synergistic effects and mechanisms by which these combinations inactivate antibiotic-resistant bacteria. In this study, two clinical strains of *S. aureus* (including one from a diabetic foot ulcer infection) were used to investigate the impact of bacterial susceptibility profiles in aPDI with Ber-Ab and Cur-Ab combinations. In addition, three antibiotics, gentamicin (Gen), mupirocin (Mup), and tobramycin (Tob) were selected based on their topical use in the treatment of *S. aureus* wound infections in clinical settings [19]. The effects on the bacterial targets were investigated by assessing ROS formation, bacterial membrane impairment, DNA damage, motility, and inhibition of virulence factors. The role of blue light irradiation in the interaction of the Ber-Ab and Cur-Ab combinations with *S. aureus* targets was also investigated.

2. Materials and methods

2.1. Bacterial strains and culture conditions

Two *S. aureus* strains were used to observe the influence of the bacterial susceptibility profile on the antibacterial mode of action of the presented strategy. *S. aureus* CECT 976 (Spanish Type Culture Collection (CECT) strain of methicillin-susceptible *S. aureus* (MSSA)) was isolated from ham implicated in a case of food poisoning. *S. aureus* MJMC568-B (clinical strain of methicillin-resistant *S. aureus* (MRSA)) was isolated from a patient with a diabetic foot ulcer during a diabetic foot consultation at the Centro Hospitalar de Trás-os-Montes e Alto Douro (Portugal). Both strains have a resistant and/or intermediate profile to Gen and Tob (MRSA resistant to Gen and Tob, MSSA resistant to Gen and intermediate to Tob). These *S. aureus* strains had already been used as model microorganisms for antimicrobial testing with antimicrobial agents [5,6]. The bacterial strains were stored at -80 °C in Mueller-Hinton Broth (MHB, Merck, Darmstadt, Germany) supplemented with 30 % glycerol (v/v, VWR, Belgium) and subcultured in MH-Agar (MHA, Merck, Darmstadt, Germany) before the experiments. For all experiments, the bacterial suspensions were grown overnight (16–18 h) in MHB at 37 °C with shaking (150 rpm, AGITORB 200, Aralab, Rio de Mouro, Portugal).

2.2. Antibiotics

The antibiotics Gen, Mup (from AppliChem, GmbH, Darmstadt, Germany; purity of 68 % and 90 %, respectively) and Tob (Tokyo chemical industry Co., ltd., Tokyo, Japan; purity > 94 %) were selected due to their topical and clinical applicability against *S. aureus* wound infections [19] (Fig. 1). The stock solutions of Gen and Tob were prepared in sterile distilled water (dH_2O) and stored in the dark at -20 °C. In the case of Mup, the stock solution was prepared in dimethyl sulfoxide (DMSO 100 %, VWR, Belgium). The proportion of DMSO never exceeded 10 % (v/v) of the final volume of the bacterial suspensions in all experiments.

2.3. PS and aPDI parameters

Ber (Cayman Chemical Company, Michigan, USA; purity ≥ 95 %) and Cur (Alfa Aesar, Karlsruhe, Germany; purity of 95 %) were the phytochemicals selected as PS (Fig. 1). These phytochemicals were purchased as pure compounds and the stock solutions were prepared in DMSO 100 % and stored in the dark at -20 °C. The proportion of DMSO never exceeded 10 % (v/v) of the final volume of the bacterial suspensions. Ber and Cur were photoactivated with a blue light-emitting diode

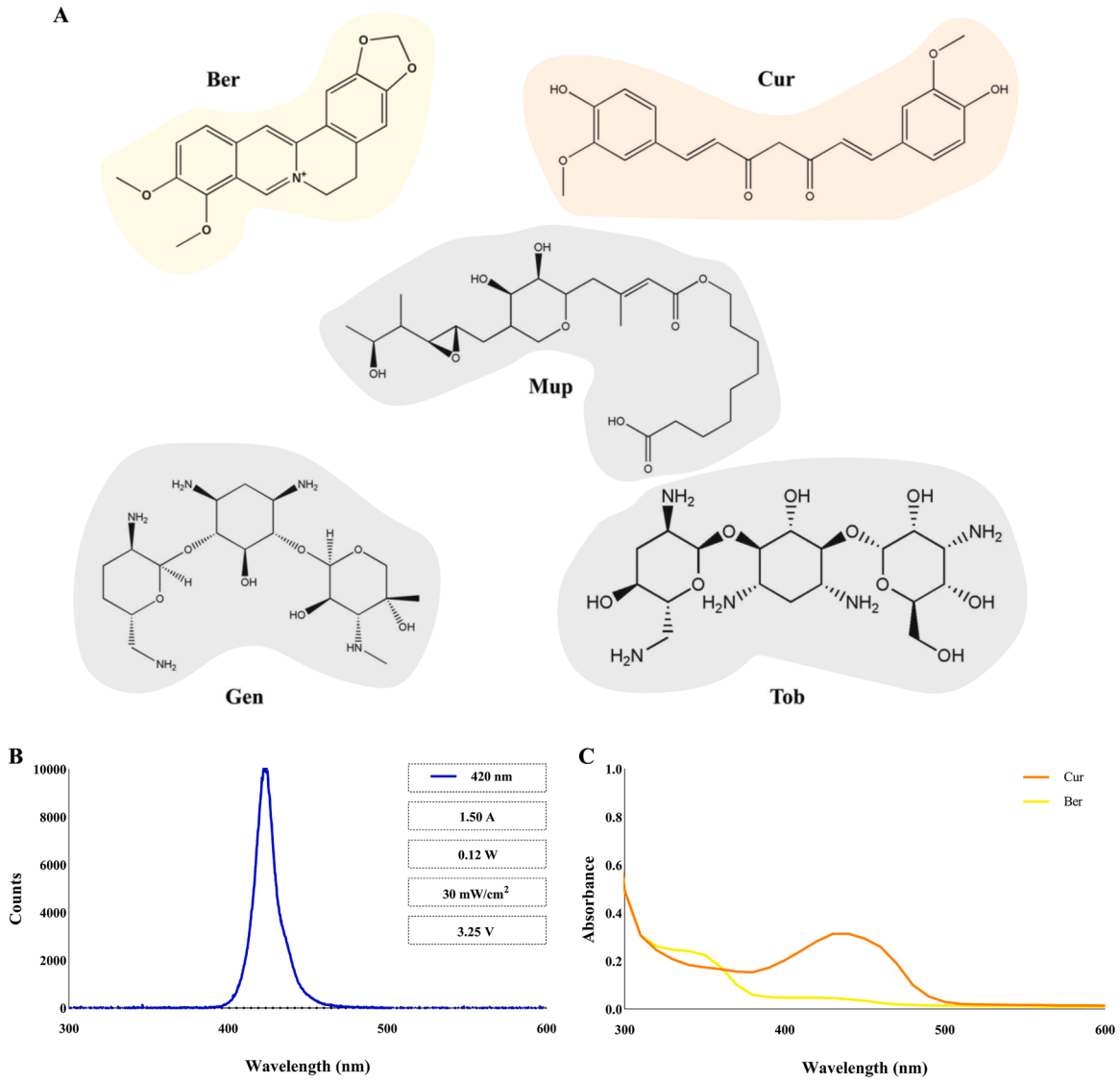

Fig. 1. LED and phytochemicals spectrum characterization. (A) Chemical structure of Ber, Cur, Gen, Mup, and Tob (obtained from ChemDraw Pro 8.0). (B) Emission spectrum of 420 nm LED. (C) UV–vis absorption spectra of Ber and Cur.

(LED) at 420 nm (30 mW/cm^2) for 10 min (18 J/cm^2, Fig. 1). The blue LED array comprises 40 individual LEDs assembled using a 96-well template. Each LED is positioned to illuminate exclusively a single well, ensuring targeted and uniform exposure in each well. To ensure accuracy and consistency across all samples, the irradiance of each LED has been carefully measured and calibrated. This configuration ensures that every sample on the test plate is exposed to the same irradiance conditions, ensuring the reliability and repeatability of test results.

2.4. Photoirradiation of Ber-Ab and Cur-Ab combinations

The antibacterial photodynamic activation of Ber-Ab and Cur-Ab combinations was performed according to Silva et al. [20], with some modifications. In brief, after overnight bacterial growth at 37 °C in MHB, bacterial cells were centrifuged (3772 × *g*, 10 min) and resuspended in sodium chloride solution (NaCl: 0.85 % v/v, VWR, Belgium) to obtain an optical density of 0.132 ± 0.02 (corresponding to 10^8 CFU/mL) at 600

Table 1
MIC and concentrations used of Ber, Cur, and antibiotics in the combinations applied as a treatment to *S. aureus* strains.

	Ber-Ab and Cur-Ab combinations	Phytochemicals		Antibiotics	
		MIC (μg/mL)	Selected concentrations (μg/mL)	MIC (μg/mL)	Selected concentrations (μg/mL)
MRSA strain	Ber-Tob	800	50	64	0.50
	Ber-Gen			>1024	0.50
	Cur-Tob	200	3.13	64	0.13
	Cur-Gen			>1024	0.50
	Cur-Mup			16	8
MSSA strain	Ber-Mup	100	6.25	8	1
	Cur-Mup	200	3.13		4
	Cur-Tob			4	0.25

nm. Subsequently, 180 μL of cells, 20 μL of Ber, Cur, Gen, Mup, Tob, and the respective Ber-Ab and Cur-Ab combinations were inoculated into 96-well polystyrene microtitre plates (Orange Scientific, BraineL'Alleud - Belgium). The Ber, Cur, Gen, Mup, and Tob concentration used were selected based on the previous statement of Gonçalves et al. [21] (Table 1). Specifically, the concentrations for the Ber-Ab and Cur-Ab combinations that achieved the most significant reductions in bacterial culturability were used as a reference for the mode of action studies on *S. aureus*. Negative controls were performed with 5 % DMSO (in the cases of the Ber and Cur combinations with Tob and Gen diluted in dH_2O) and 10 % (Ber-Mup and Cur-Mup combinations) and with bacterial cells exposed or not exposed to blue light irradiation. Positive controls were performed using H_2O_2 at 3 % (v/v), Ber at 800 (for MRSA) and 100 μg/mL (for MSSA), and Cur at 200 μg/mL (for both MRSA and MSSA). H_2O_2 was chosen to evaluate its influence on ROS production and its possible impact on the other mechanisms of action investigated due to its known effects in this regard [22]. Considering the known efficacy of Ber and Cur in affecting membrane integrity, DNA damage, and impairment of bacterial virulence, these phytochemicals were used at concentrations higher than the selected for the tests (at minimum inhibitory concentrations (MIC)) [14,15,23–27]. The plates were then incubated at 37 °C for 30 min, at 150 rpm in the dark. The cells were then irradiated for 10 min with a 420 nm LED at 30 mW/cm^2 under a laminar flow hood in the dark. The control groups received no irradiation treatment. After irradiation, an incubation period of 6 h at 37 °C, 150 rpm, and in the dark was performed. As topical antibiotics are usually applied 2–3 times a day [28] to maximize their effectiveness, an incubation period of 6 h following irradiation was implemented. This 6 h incubation period also simulates a realistic topical application of aPDI for acute skin wound infections. Subsequently, the targets of antibacterial activity were investigated by evaluating the combined effects of photo- and non-photoactivated optimized Ber-Ab and Cur-Ab concentrations on different bacterial physiological indices: Generation of ROS, alteration of membrane integrity through propidium iodide (PI) uptake, potassium (K^+) leakage and alteration of bacterial surface charge, DNA damage, inhibition of motility and production of virulence factors as total proteases (Prot), gelatinases (Gel) and lipases (Lip).

2.5. Assessment of the antibacterial mode of action

2.5.1. ROS generation

The generation of intracellular ROS was measured using the probe 2,7-dichlorodihydrofluorescein diacetate (DCF-DA, Alfa Aesar, Karlsruhe, Germany), as described by Zhang et al. [29]. DCF-DA was used as a fluorescent probe to detect the intracellular ROS content [30]. After 6 h of incubation, the DCF-DA probe was added to all conditions at a final concentration of 10 μM and incubated in the dark at 37 °C for 30 min under agitation (150 rpm). DCF-DA fluorescence (λ_{ex} = 488 nm and λ_{em} = 540 nm) was quantified using a microplate reader (Synergy HT, Biotek, Winooski, VT, USA).

2.5.2. Membrane integrity

2.5.2.1. PI uptake. The Live/Dead BacLightTM Viability Kit was used to assess the integrity of cell membranes according to Borges et al. [31]. This kit contains two nucleic acid-binding dyes, SYTO9™ and PI, which allows the determination of membrane integrity by selective dye exclusion. SYTO9™ (green bloomdye) can penetrate all bacterial cells and stains the cells green, while PI (red dye) can penetrate only the bacterial cells with damaged membrane and bind to double-stranded DNA, resulting in red-stained fluorescence cells [31]. After 6 h of incubation, a volume of 700 μL of each bacterial suspension was stained with 250 μL SYTO9™ and 50 μL PI and allowed to react in the dark for 7 min. Then, the mixture was filtered through a black 0.22 μm polycarbonate nucleopore membrane (Whatman International Ltd., Maidstone, UK). Finally, the membranes were mounted on a microscope slide and the samples were observed in a LEICA DMLB2 epifluorescence microscope (LEICA Microsystems Ltd., Weltzlar, Germany) using ultraviolet light. The optimal optical filter combination for viewing stained mounts is a 480–500 nm excitation filter paired with a 485 nm emission filter (Chroma 61,000-V2 DAPI/FITC/TRITC). In addition, a Leica DFC300 FX camera was connected to the microscope and a 100 × oil immersion fluorescence objective was used. The total number of cells and the number of PI-stained cells on each polycarbonate membrane were determined using 20 fields of view. The number of cells with intact (green) and damaged (red) membranes *per* mL of sample was calculated using the following Eq. (1):

$$N = \frac{n \times A}{B \times V} \times D \quad (1)$$

where N is the number of cells in the sample *per* mL, n is the average number of cells per microscopic field, A is the membrane area (cm^2), B is the microscopic field area (cm^2), V is the sample volume filtered (mL) and D is the dilution factor.

2.5.2.2. Intracellular K^+ leakage. Flame emission and atomic absorption spectroscopy were used for K^+ titration in solutions of the bacterial suspensions [31]. After 6 h of incubation, samples were collected, filtered and then analysed on a GBC AAS Device 932plus using GBC Avante 1.33 software (GBC Scientific Equipment, Hampshire, IL, USA).

2.5.2.3. Bacterial surface charge change. The zeta potential of bacterial suspensions, after 6 h of incubation, was determined using a Nano Zetasizer (Malvern Instruments) [31]. Zeta potential was measured by applying an electric field through the bacterial suspensions.

2.5.3. DNA damage

Bacterial DNA damage was assessed by flow cytometry by the detection of intact DNA using PI (from the Live/Dead BacLightTM Viability Kit), according to Gao et al. [32], with some modifications. In brief, after 6 h of incubation, all bacteria were centrifuged (3772 × *g*, 10 min**)** and resuspended in 500 mL ethyl alcohol (VWR, Belgium) 50 % to permeabilize the membrane. After 30 min at -20 °C, all conditions were centrifuged and resuspended in 500 mL dH_2O and 100 μL PI at 10 μg/mL was added. After 30 min, the cells were centrifuged and resuspended in dH_2O. Samples were analysed with CytExpert software (version 2.4.0.28, Beckman Coulter, Brea, CA, USA) in a CytoFLEX flow cytometer, model V0-B3-R1 (Beckman Coulter, Brea, CA, USA), through filter PC5.5-A (λex = 488 nm, λem = 665–715 nm). DNA fragmentation was observed by the decrease in PI fluorescence. It should be noted that this test only allows the observation of double-stranded DNA breaks. Since PI cannot bind to broken DNA chains, the decrease in PI fluorescence correlates directly with the decrease in double-stranded DNA content. To confirm this, additional measurements were conducted using acridine orange (AO, Panreac; Montplet & Esteban S.A., Barcelona, Spain), following the method of Diaper et al. [33], with some modifications. Briefly, after permeabilization with ethyl alcohol, all samples were centrifuged and resuspended in 500 μL of dH_2O. Subsequently, 100 μL of AO at a concentration of 10 μg/mL was added. The samples were incubated for 15 min, centrifuged again, and resuspended in dH_2O. Analysis was performed using CytExpert software through the FITC filter (λex=488 nm, λem=525±40 nm). AO emits green fluorescence when bound to double-stranded DNA and orange when it interacts with single-stranded nucleic acids or RNA [34]. The measurement of green fluorescence allows the assessment of DNA integrity, with a decrease in signal indicating damage. This dual-dye approach provides complementary evidence, strengthening the reliability of the observed DNA damage.

2.5.4. Motility inhibition

The inhibition of bacterial motility of both *S. aureus* strains was evaluated as described by Borges et al. [35]. *S. aureus* spreads on soft agar plates through sliding motility. For this purpose, after 6 h of incubation, 15 μL of the bacterial suspension was added to the center of agar plates containing 10 g/L (1 %) tryptone (Merck, Darmstadt, Germany), 2.5 g/L (0.25 %) NaCl (VWR, Belgium) and 3 g/L (0.30 %) agar (VWR, Belgium). The plates were incubated at 37 °C and the diameter (mm) of the bacterial motility halos was measured after 24, 48, and 72 h.

2.5.5. Inhibition of virulence factors

Inhibition of factors associated with virulence of both *S. aureus* strains was assessed after 6 h by measuring total Prot production, as well as Lip and Gel activity. The production of total Prot was assessed as described by Abdelmotele et al. [36]. In brief, after 6 h of incubation, 10 μL of each condition was added to Petri dishes containing plate count agar (PCA; VWR, Belgium) with 10 g/L (1 %) of skim milk powder (Merck, Darmstadt, Germany) and incubated at 37 °C for 72 h. The presence of clearance zones indicated the production of total Prot. Lip production was determined according to Meheissen et al. [37]. After the exposure time, 10 μL of each bacterial suspension was added to agar plates containing 2 g/L (0.20 %) $CaCl_2$ (Merck, Darmstadt, Germany), 15 g/L (1.50 %) agar (VWR, Belgium), 20 g/L (2 %) Luria-Bertani broth (LBB; Sigma-Aldrich, St. Louis, MO, USA) and 9.44 mL/L Tween 80 0 (VWR, Belgium). The plates were incubated at 37 °C for 48 h. Lip production was detected by the appearance of a light-yellow clear halo around the bacterial colony. Gel activity was evaluated using the method described by Lopes et al. [38]. For this purpose, after 6 h of incubation, 10 μL of each condition was plated out on Petri dishes containing gelatine agar (5 g/L peptone (0.50 %) (Merck, Darmstadt, Germany), 3 g/L (0.30 %) yeast extract (Oxoid, United Kingdom), 30 g/L (3 %) gelatine (Oxoid, United Kingdom), 15 g/L (1.50 %) agar (VWR, Belgium). After 48 h at 37 °C, the plates were flooded with a saturated solution of ammonium sulphate (VWR, Belgium). Gel production was observed through a transparent halo around the colony.

2.6. Combinatorial index of Ber-Ab and Cur-Ab

The interaction between the different combinations of Ber and Cur was scored using the ∑ Combinatorial Index (∑CI) proposed by Baptista et al. [39]. The combinatorial index for Ber and Cur (CI_{Phy}) was calculated according to Eq. (2):

$$CI_{Phy} = \frac{VPhy}{VPhy + Ab} \quad (2)$$

Where V_{Phy} represents the values obtained for Ber and Cur individually for each method (ROS formation, bacterial membrane integrity, DNA damage, motility, and virulence factor production), and V_{Phy+Ab} denotes the results obtained from the use of Ber-Ab and Cur-Ab combinations and for each method.

The evaluation of the antibiotic Combinatorial Index (CI_{Ab}) followed a similar approach. The sum of CI_{Phy} and CI_{Ab} then gives ΣCI, as shown in Eq. (3):

$$\sum CI = CI_{Phy} + CI_{Ab} \quad (3)$$

The ΣCI values calculated were further classified based on the interaction between the phytochemicals (Ber and Cur) and the antibiotics (Tob, Gen, and Mup). Values lower than 0.5 indicate a synergistic effect (+++), between 0.5 and 2 indicate an additive effect (++), between 2 and 4 is categorized as an indifferent effect (+), and higher than 4 indicates an antagonistic effect (-).

2.7. Statistical analysis

The mean ± standard deviation (SD) of each sample were calculated. Experimental data were analysed with the statistical program GraphPad Prism 8.0.1 for Windows (GraphPad Software, La Jolla, California, USA) using one-way ANOVA multiple comparisons. Statistical differences were determined for a probability level of 95 % ($P < 0.05$; * $P < 0.05$, ** $P < 0.01$, *** $P < 0.001$, **** $P < 0.0001$). All experiments were performed in duplicate with at least three replicates *per* condition.

3. Results

3.1. Antibacterial mode of action of blue light photoactivated and non-photoactivated Ber-Ab and Cur-Ab combinations

To study the effects on the different bacterial targets, Ber-Ab and Cur-Ab were used at selected concentrations (Table 1) obtained in a previous study [21]. The combinations of Ber-Ab and Cur-Ab that resulted in complete inhibition of culturability were selected to evaluate the antibacterial mode of action.

3.1.1. Ber-Ab and Cur-Ab combinations ROS generation profile

The ROS production capacity of both photoactivated and non-photoactivated Ber-Ab and Cur-Ab combinations, along with their respective compounds, is presented in Fig. 2. The intensity of the DCF-DA probe directly correlates with ROS levels, as DCF-DA binds to ROS and emits fluorescence, allowing the quantification of ROS production.

ROS production was observed in the negative controls (bacterial cells, DMSO 5 % and 10 %) for both *S. aureus* strains, although at significantly lower levels compared to the positive controls (H_2O_2 at 3 % v/v, Ber at 800 μg/mL for MRSA and 100 μg/mL for MSSA and Cur at 200 μg/mL). Treatment with antibiotics led to a small increase in ROS levels in both strains compared to the untreated bacterial cells ($P < 0.05$). Nevertheless, a significant decrease in ROS levels was observed with low concentrations of Mup (of the MRSA strain, Fig. 2**B**) and Tob (at 0.13 μg/mL of the MSSA strain, Fig. 2**D**) after photoactivation ($P < 0.05$). Photoactivated Mup at a concentration of 8 μg/mL exhibited an opposite effect on the MRSA strain and led to increased ROS levels ($P < 0.05$). In the case of non-photoactivated Ber and Cur alone, a slight increase in ROS production was observed in both strains (except for Ber at 50 μg/mL in the MRSA strain), although the effect was more pronounced in the MSSA strain (Cur at 3.13 μg/mL, $P < 0.05$, Fig. 2**D**). Furthermore, photoactivation of Ber and Cur with blue light resulted in a notable increase in ROS levels, specifically for Cur at 3.13 μg/mL in the MRSA strain ($P < 0.05$, Fig. 2**B**). Non-photoactivated Ber-Ab and Cur-Ab combinations (except Cur-Gen and Cur-Mup combinations in MRSA) promoted lower ROS formation in both strains than their respective compounds alone. However, blue light photoactivation of the Ber-Ab (Fig. 2**A** and **C**) and Cur-Ab (Fig. 2**B** and **D**) combinations resulted in an increased capacity for ROS production compared to their non-photoactivated counterparts.

To understand the combined effect of Ber-Ab and Cur-Ab combinations, the ∑CI scoring in **Table S4** was analysed. These combinations without irradiation led to an antagonistic effect (-) in both Ber-Ab combinations and to an additive effect (++) in Cur-Gen and Cur-Mup of the MRSA strain, while all Ber-Ab and Cur-Ab combinations led to an indifferent effect (+) against the MSSA strain. Nonetheless, upon photoactivation, all combinations demonstrated increased ROS production capacity compared to the photoactivated individual compounds ($P < 0.05$), resulting in an additive effect (++).

3.1.2. Effect of Ber-Ab and Cur-Ab combinations on membrane integrity

3.1.2.1. Influence on PI uptake. Non-photoactivated positive controls (H_2O_2 at 3 % v/v, Ber at 800 μg/mL for MRSA and 100 μg/mL for MSSA and Cur at 200 μg/mL) resulted in a significant membrane damage for both *S. aureus* strains. However, blue light irradiation increased this effect only for H_2O_2 ($P < 0.05$). On the other hand, blue light irradiation

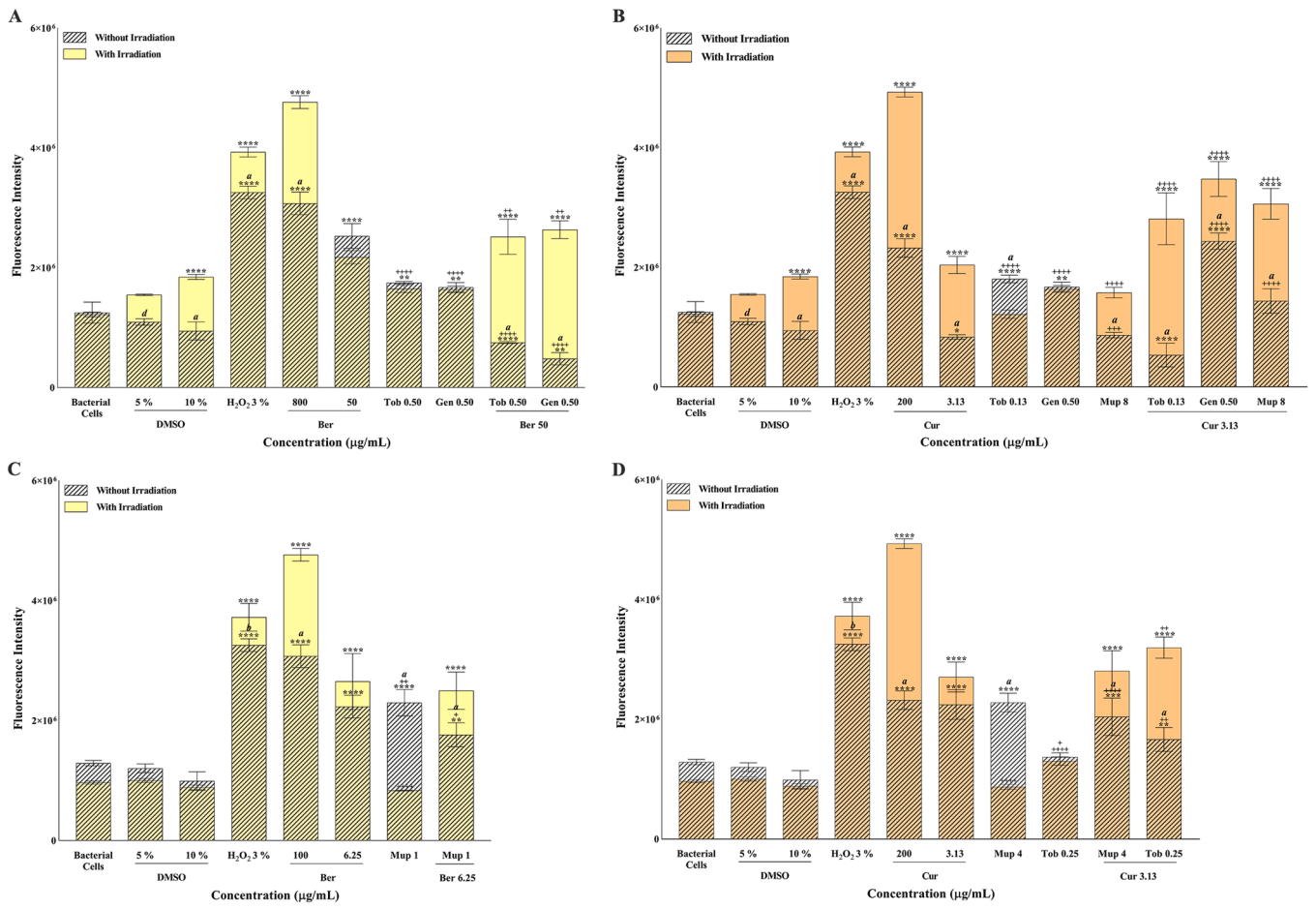

Fig. 2. ROS production assessed by DCF-DA fluorescent probe after treatment of MRSA (A and B) and MSSA (C and D) strains with the combination of Ber (A and C) or Cur (B and D) with several antibiotics (Mup, Tob, and Gen) at different concentrations, under irradiation and darkness conditions. Data are presented as mean ± SDs for two independent experiments with at least three replicates. *a* stands for ****, *b* stands for ***, *c* stands for ** and *d* stands for *. Statistical analyses were performed between irradiated and non-irradiated groups (represented by the letters above the bars) and compared to bacterial cells without irradiation (represented by the * above the bars). Additionally, a statistical analysis comparing Ber, Cur, Tob, Gen, and Mup alone and combined in respective combinations was performed (represented by + above the bars).

alone and DMSO (5% and 10%) exhibited no significant effect on the membrane integrity of MSSA ($P > 0.05$, Fig. 3). In the case of MRSA strain, DMSO (5 % and 10 %) showed a slight decrease in membrane integrity ($P < 0.05$, Fig. 4).

Regarding the MSSA strain (Fig. 3), non-photoactivated Ber and Cur alone promoted a significant increase in membrane damage ($P < 0.05$). Blue light photoactivation of Ber and Cur alone significantly enhanced their membrane damage ability ($P < 0.05$). In the case of Mup and Tob, photoactivation showed no significant effect ($P > 0.05$), except Mup (at 1 μg/mL), where a slight decrease in the percentage of cells stained with PI was observed. The percentage of cells stained with PI was higher with photoactivated Ber-Ab and Cur-Ab combinations than with Ber, Cur, and the antibiotics alone ($P < 0.05$, Fig. 3). Nevertheless, the non-photoactivated Ber-Ab and Cur-Ab combinations had a lower effect than the respective compounds alone.

In the case of the MRSA strain (Fig. 4), non-photoactivated Ber and Cur did not demonstrate any effect on membrane integrity ($P > 0.05$), whereas their photoactivated counterparts significantly damaged the membrane ($P < 0.05$). An increase in PI-stained cells was observed when the antibiotics Tob (at 0.50 μg/mL), Gen, and Mup were used, whether with or without photoactivation. The photoactivated Ber-Ab combinations (Ber-Tob and Ber-Gen) promoted the highest reduction in membrane integrity (≈ 90 %), while the same non-photoactivated conditions resulted in a percentage of PI permeabilization close to 50 %. Moreover, Tob and Gen (at 0.50 μg/mL) alone caused only ≈ 10 % of PI permeabilization. Photoactivated Cur-Tob and Cur-Gen combinations also showed a high ability to damage the membrane of the MRSA strain (≈ 60 % and 40 %, respectively). However, non-photoactivated and photoactivated Cur-Mup showed the lowest ability to increase MRSA membrane damage (≈ 25 %).

The percentage of cells with damaged membranes was more pronounced in the MRSA strain (Fig. 4**A** and **B**) than in that MSSA (Fig. 3**A** and **B**). While only about 40 % of the MSSA cells were stained with PI, *circa* 90 % of the MRSA cells were stained with PI. Figs. 3**C, 4 C,** and Fig. 5 show that photoactivated Ber-Ab and Cur-Ab combinations significantly decreased the number of total cells in comparison to the non-photoactivated conditions.

The $\sum$ CI scoring in **Table S4** demonstrated that although non-photoactivated Ber and Cur did not exhibit increased membrane damage, the non-photoactivated Ber-Ab and Cur-Ab combinations showed an additive (Cur-Mup for both strains) and a synergistic (Ber-Tob, Ber-Gen and Cur-Tob in MRSA) effect. In de case of photoactivated Ber-Ab and Cur-Ab combinations, an overall additive effect (++) was observed (except Cur-Tob and Cur-Gen in the MRSA strain, which resulted in a synergistic effect (+++)).

3.1.2.2. Interference with intracellular K^+ release. Non-photoactivated positive controls (H_2O_2 at 3 % v/v, Ber at 800 μg/mL for MRSA and 100 μg/mL for MSSA and Cur at 200 μg/mL) significantly increased the K^+ release by both *S. aureus* strains ($P < 0.05$) (**Table S1**). Irradiation

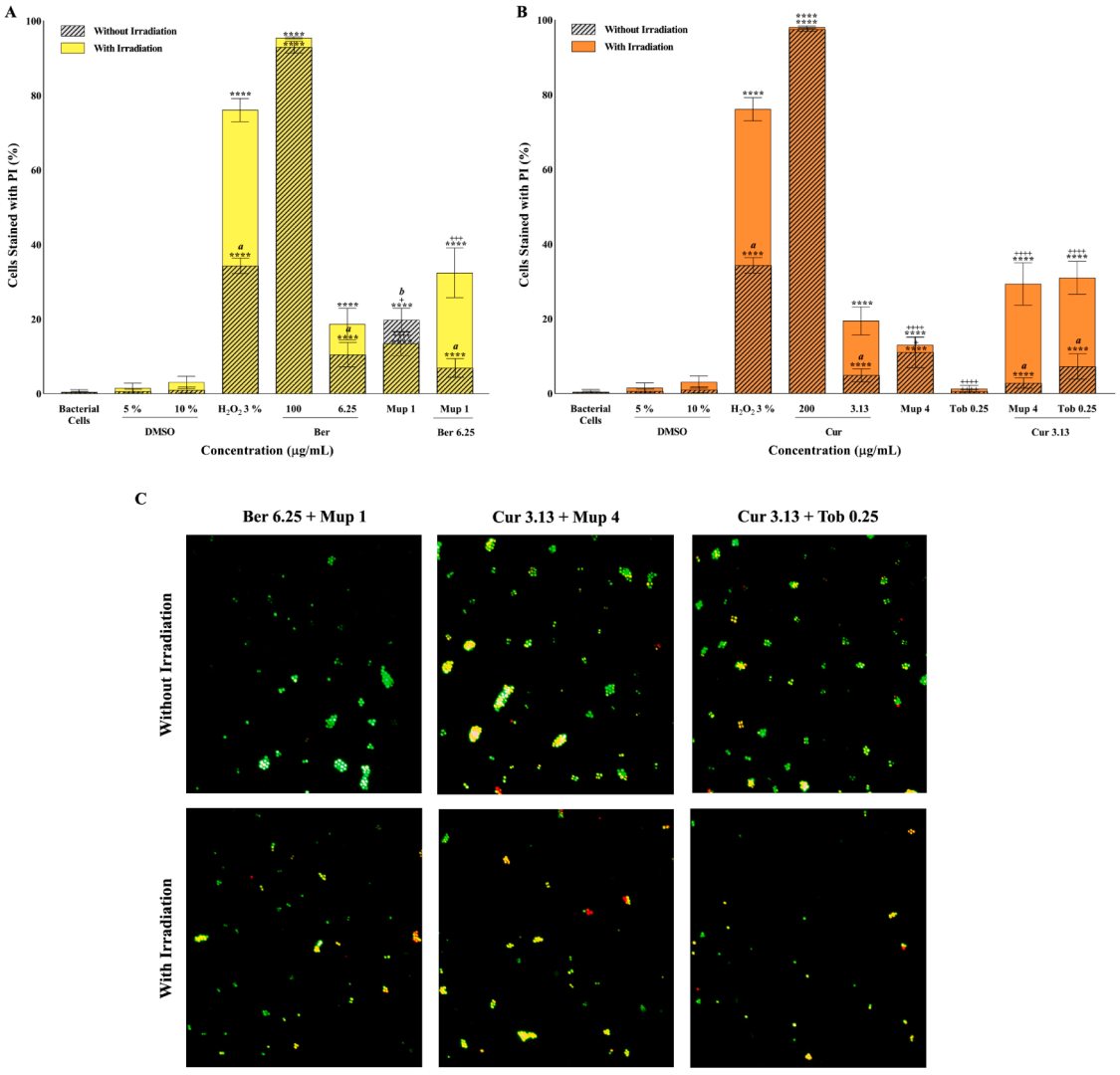

Fig. 3. Membrane integrity evaluated by PI uptake of MSSA strain after Ber-Ab (A) and Cur-Ab (B) combinations treatment, under irradiation and darkness conditions. Percentage of cells stained with PI using different concentrations of Ber-Ab and Cur-Ab combinations. (C) Illustrative examples of photoactivated and non-photoactivated Ber-Mup, Cur-Mup, and Cur-Tob combinations (The scale bar corresponds to 10 µm). Data are presented as mean ± SDs for two independent experiments with at least three replicates. *a* stands for ****, *b* stands for ***, *c* stands for ** and *d* stands for *. Statistical analyses were performed between irradiated and non-irradiated groups (represented by the letters above the bars) and compared to bacterial cells without irradiation (represented by the * above the bars). Additionally, a statistical analysis comparing Ber, Cur, Tob, Gen, and Mup alone and combined in respective combinations was performed (represented by + above the bars).

improved the ability of positive controls to increase intracellular K^+ release ($P < 0.05$). DMSO (5% and 10%) exhibited a significant impact on K^+ release for both strains ($P < 0.05$), especially for MRSA (**Table S1**). Similarly, photoactivation promoted increased K^+ release ($P < 0.05$). Furthermore, non-photoactivated phytochemicals and antibiotics alone led to significant K^+ release from both strains compared to positive controls ($P < 0.05$). In general, blue light photoactivation of all compounds tested when used alone improved their K^+ release capacity for both strains ($P < 0.05$). Notably, photoactivation of Ber-Ab and Cur-Ab combinations significantly enhanced K^+ release from both strains, particularly when compared to non-photoactivated conditions ($P < 0.05$) and the positive controls (**Table S1**).

Based on the $\sum$ CI scoring (**Table S4**), all photoactivated Ber-Ab and Cur-Ab combinations led to an additive effect (++) on both *S. aureus* strains.

3.1.2.3. Action on bacterial surface charge. Both strains without any treatment had a negative surface charge: -16.76 ± 1.34 mV for the MRSA and -18.89 ± 0.95 mV for the MSSA (**Table S1**). Nonetheless, after treatment with positive controls (H_2O_2 at 3 % v/v, Ber at 800 µg/mL for MRSA and 100 µg/mL for MSSA, and Cur at 200 µg/mL), the zeta potential of both strains changed to less negative values ($P < 0.05$) (**Table S1**). Furthermore, blue light irradiation of positive controls amplified this effect ($P < 0.05$). In contrast, photoactivated Ber-Ab and Cur-Ab combinations, as well as their respective compounds alone, resulted in minor decreases in cell surface charge (approximately 2-3 mV, $P < 0.05$) in both *S. aureus* strains. Furthermore, non-photoactivated Ber-Ab and Cur-Ab combinations did not show any improvement compared to their respective compounds alone (**Table S1**).

Based on the $\sum$ CI scoring (**Table S4**), non-photoactivated Ber-Tob, Ber-Gen and Cur-Tob and photoactivated Ber-Gen, Cur-Tob, and Cur-Gen combinations had an indifferent effect (+) on MRSA. In contrast, only the photoactivated and non-photoactivated Cur-Mup had an indifferent effect (+) on MSSA, while the other photoactivated and non-photoactivated combinations had an additive effect (++).

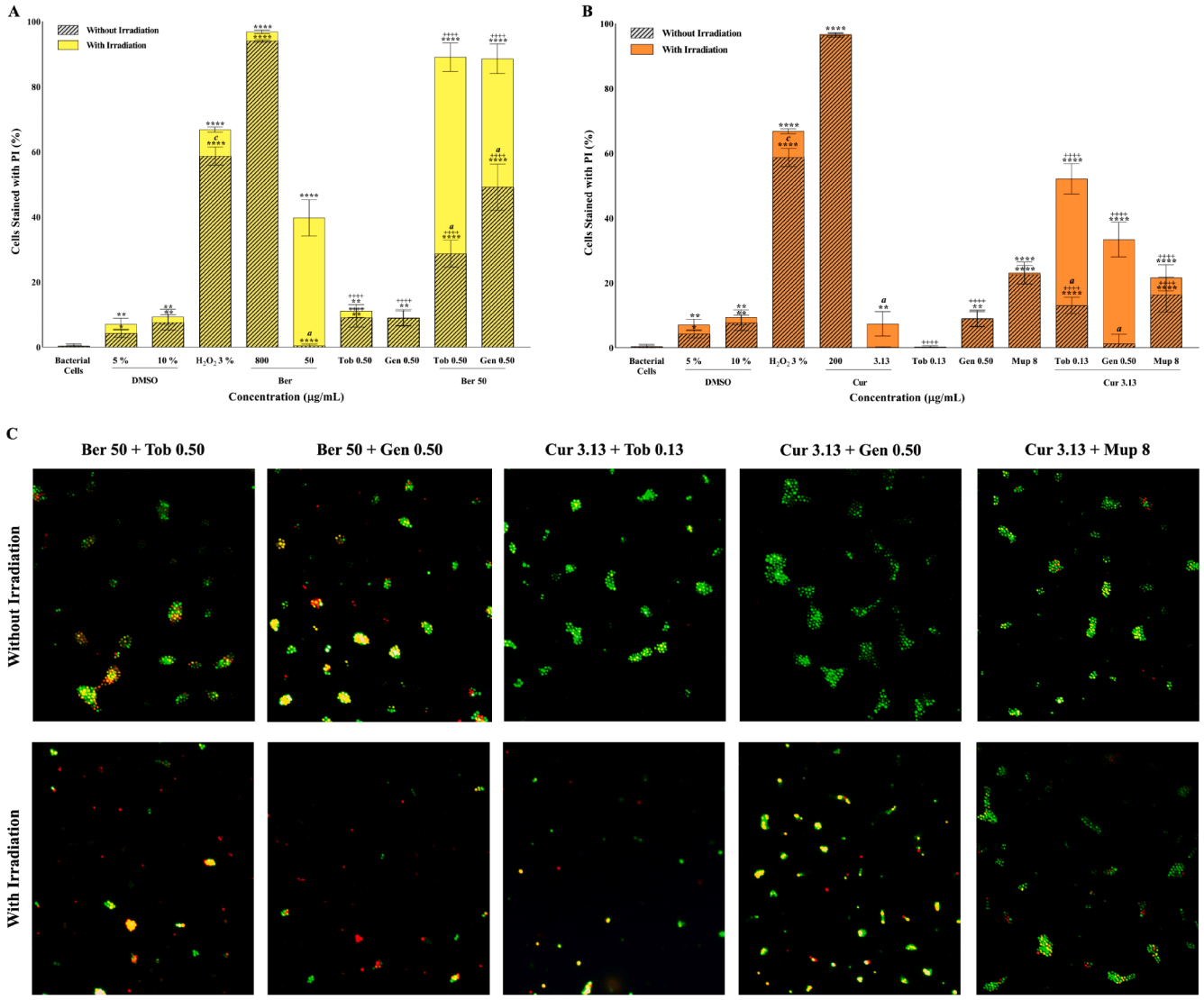

Fig. 4. Membrane integrity evaluated by PI uptake of MRSA strain after Ber-Ab (A) and Cur-Ab (B) combinations treatment, under irradiation and darkness conditions. Percentage of cells stained with PI using different concentrations of Ber-Ab and Cur-Ab combinations. (C) Illustrative examples of photoactivated and non-photoactivated Ber-Tob, Ber-Gen, Cur-Mup, Cur-Gen and Cur-Tob combinations (The scale bar corresponds to 10 µm). Data are presented as mean ± SDs for two independent experiments with at least three replicates. *a* stands for ****, *b* stands for ***, *c* stands for ** and *d* stands for *. Statistical analyses were performed between irradiated and non-irradiated groups (represented by the letters above the bars) and compared to bacterial cells without irradiation (represented by the * above the bars). Additionally, a statistical analysis comparing Ber, Cur, Tob, Gen, and Mup alone and combined in respective combinations was performed (represented by + above the bars).

3.1.3. *Effect of Ber-Ab and Cur-Ab combinations on DNA damage*

Non-photoactivated positive controls (H_2O_2 at 3 % v/v, Ber at 800 µg/mL for MRSA and 100 µg/mL for MSSA and Cur at 200 µg/mL) significantly increased the DNA damage of both *S. aureus* strains ($P < 0.05$) (Fig. 6). Furthermore, blue light irradiation increased this effect for all positive controls used ($P < 0.05$). On the other hand, irradiation alone and DMSO (5% and 10%) had no significant effect on DNA damage of both strains ($P > 0.05$). Analysis of PI and AO fluorescence revealed consistent trends for the DNA-double strand damaging effects of the compounds tested. Non-photoactivated Ber caused no significant DNA damage in MRSA ($P > 0.05$, Fig. 6**A** and **C**), but caused significant damage in MSSA, as shown by AO fluorescence under photoactivation conditions ($P < 0.05$, Fig. 6**G**). Similarly, Cur alone did not exhibit significant DNA-damaging effects in MSSA based on PI staining ($P > 0.05$, Fig. 6**F**), while AO staining showed significant DNA damage, especially under photoactivation ($P < 0.05$, Fig. 6**H**). All antibiotics tested without irradiation induced DNA damage in both strains ($P < 0.05$). Blue light irradiation did not significantly enhance DNA damage for most compounds alone ($P > 0.05$), except Ber and Mup in MSSA and MRSA strains ($P < 0.05$), respectively. However, both PI and AO analyses confirmed that blue light-based photoactivation enhanced the ability of all Ber-Ab and Cur-Ab combinations to induce DNA damage in both strains ($P < 0.05$), except for Cur-Mup in the MRSA strain ($P > 0.05$).

According to the $\sum$ CI scoring (**Table S4**), both non-photoactivated and photoactivated combinations of Ber-Ab and Cur-Ab showed an additive effect (++), compared to the respective compounds alone, in both strains and methods (PI and AO).

3.1.4. *Effect of Ber-Ab and Cur-Ab combinations on bacterial motility inhibition*

Both *S. aureus* strains presented an increase in sliding motility over

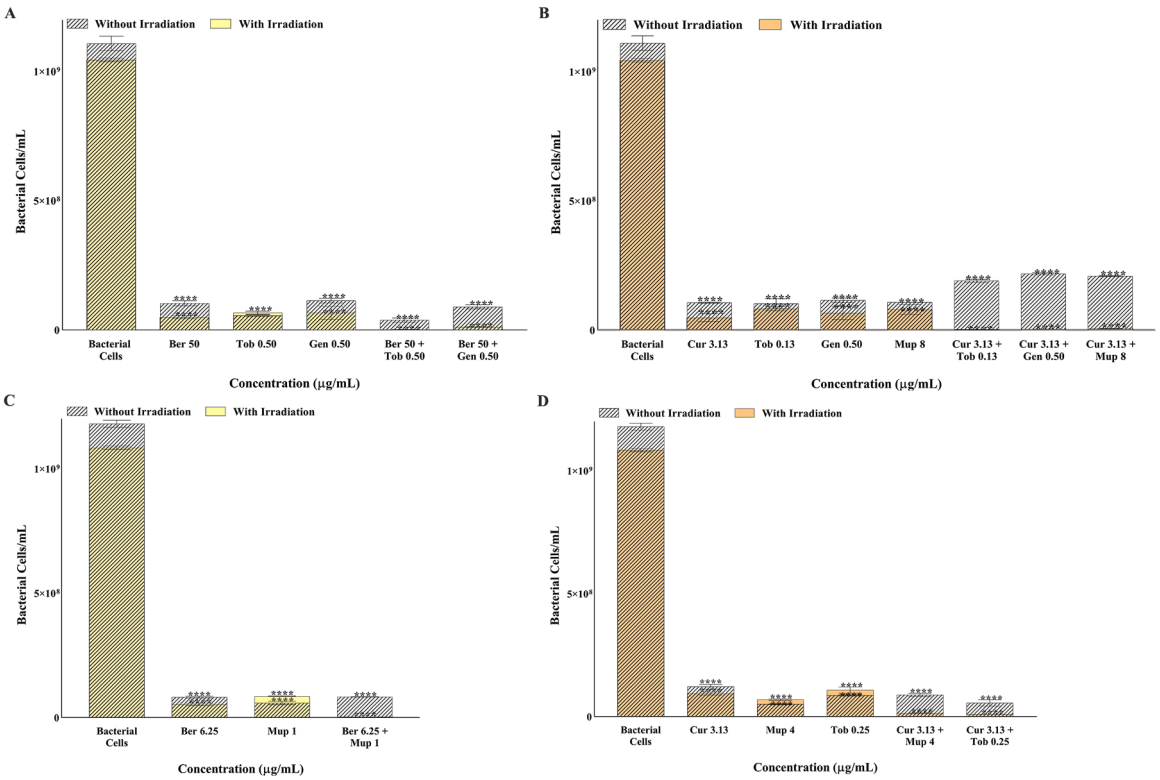

Fig. 5. Total bacterial cells *per* mL of MRSA (A and B) and MRSA (C and D) strains after Ber-Ab (A and C) and Cur-Ab (B and D) combinations treatment, under irradiation and darkness conditions. Data are presented as mean ± SDs for two independent experiments with at least three replicates. Statistical analyses were performed compared to bacterial cells without irradiation (represented by * above the bars).

time. However, the motility of both *S. aureus* strains decreased significantly over time ($P < 0.05$) for all non-photoactivated positive controls (H_2O_2 at 3 % v/v, Ber at 800 μg/mL for MRSA and 100 μg/mL for MSSA and Cur at 200 μg/mL) (**Table S2**). Irradiation with blue light showed no improvement in motility reduction in the positive controls ($P > 0.05$). Likewise, blue irradiation alone and DMSO (5% and 10%) had no significant effect on the motility of the *S. aureus* strains. Nonetheless, a significant decrease in motility was observed for most photoactivated and non-photoactivated Ber-Ab and Cur-Ab combinations (Fig. 7) ($P < 0.05$), compared to the positive controls. All combinations tested significantly reduced the motility of MRSA after 24 h (Fig. 7**A** and **B**, $P < 0.05$), but only the photoactivated combinations were able to maintain this reduction up to 72 h. Among the photoactivated combinations, Cur-Tob in MRSA showed the lowest reduction performance compared to the other combinations. Conversely, photoactivated Ber-Tob and Cur-Mup in MRSA maintained the same effect over a longer period ($P < 0.05$). In MSSA (Fig. 7**C** and **D**), all combinations significantly reduced motility over time ($P < 0.05$), with no significant differences between irradiated and non-irradiated combinations ($P > 0.05$), suggesting that photoactivation does not play a critical role in this strain.

Based on the $\sum$ CI scoring (**Table S4**), all combinations of Ber-Ab and Cur-Ab had an additive effect (++) on both *S. aureus* strains, except non-photoactivated Ber-Gen, Cur-Tob, and Cur Mup and photoactivated Ber-Tob on the MRSA strain which had a synergistic effect (+++).

3.1.5. *Effect of Ber-Ab and Cur-Ab combinations on the production of virulence factors*

The total halo, which includes bacterial growth and virulence factor production halo, and the halo of virulence factor production were measured for all conditions (**Table S3**). The results showed that both strains (without treatment) produced Prot (which was higher in the MRSA strain than in the MSSA strain), while the production of Lip and Gel was specifically observed only in the MRSA strain.

The non-photoactivated positive controls (H_2O_2 at 3 % v/v, Ber at 800 μg/mL for MRSA and 100 μg/mL for MSSA and Cur at 200 μg/mL) significantly decreased the production of virulence factors by both *S. aureus* strains ($P < 0.05$). Irradiation with blue light showed no improvement in the activity of positive controls in reducing the production of virulence factors ($P > 0.05$). Similarly, no decrease in the production of virulence factor was observed with blue light irradiation alone. Furthermore, most non-photoactivated Ber-Ab and Cur-Ab combinations, as well as the respective compounds alone, did not alter the production of virulence factors. Some conditions should be highlighted due to their more noticeable activity (Fig. 8). In the MSSA strain (Fig. 8**C** and **D**), Mup and Cur alone showed the best anti-virulence activity, compared to the positive controls. In addition, all Ber-Ab and Cur-Ab combinations effectively inhibited the production of total Prot ($P < 0.05$). On the other hand, blue light irradiation did not increase the reduction of total Prot production by non-photoactivated Ber-Ab and Cur-Ab combinations. Even though, based on the $\sum$ CI scoring (**Table S4**) all photoactivated and non-photoactivated combinations had an additive effect (++). In MRSA (Fig. 8**A** and **B**), photoactivated Cur-Gen and Cur-Mup were effective in reducing or completely inhibiting total Prot production (in the case of Cur-Mup), compared to the positive controls. Similar to the MSSA strain, in the MRSA strain all photoactivated and non-photoactivated combinations exhibited an additive effect (++). Regarding Gel production (Fig. 8**G** and **H**), all non-photoactivated Ber-Ab and Cur-Ab combinations and respective compounds alone do not affect significantly the production of Gel ($P > 0.05$). Conversely, all photoactivated Ber-Ab and Cur-Ab combinations inhibited Gel production ($P < 0.05$), resulting in a synergistic effect (+++), compared with the respective compounds alone (**Table S4**). Concerning Lip production, non-photoactivated Cur-Mup achieved a significant reduction ($P < 0.05$). Additionally, blue light irradiation enhanced the activity of certain Ber-Ab and Cur-Ab combinations in

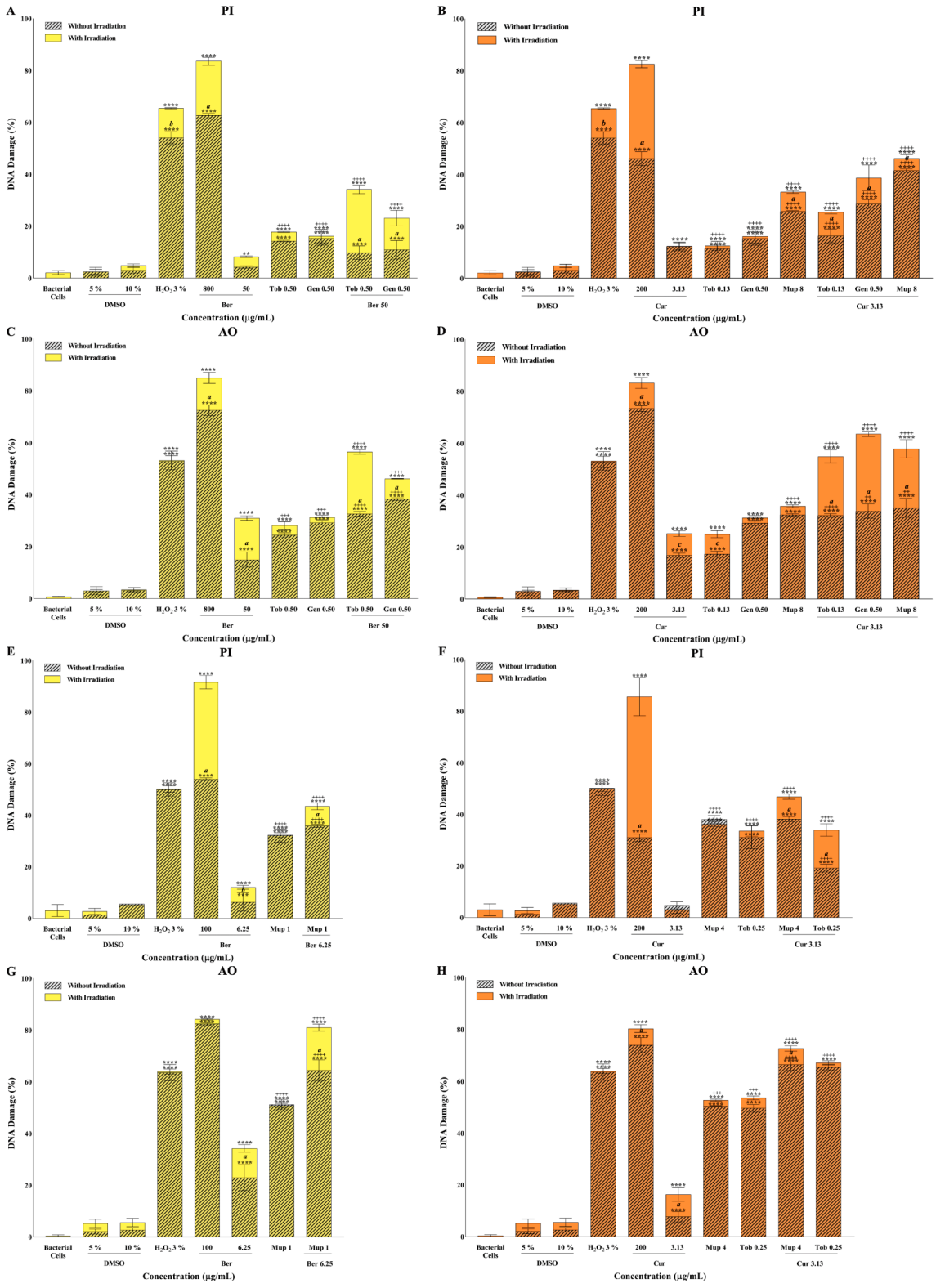

Fig. 6. DNA damage assessed by PI (A, B, E and F) and AO (C, D, G, and H) intensity fluorescence of MRSA (A, B, C, and D) and MSSA (E, F, G, and H) strains after Ber-Ab (A, C, E, and G) and Cur-Ab (B, D, F, and, H) combinations treatment at different concentrations, under irradiation and darkness conditions. Data are presented as mean ± SDs for two independent experiments with at least three replicates. *a* stands for ****, *b* stands for ***, *c* stands for ** and *d* stands for *. Statistical analyses were performed between irradiated and non-irradiated groups (represented by the letters above the bars) and compared to bacterial cells without irradiation (represented by the * above the bars). Additionally, a statistical analysis comparing Ber, Cur, Tob, Gen, and Mup alone and combined in respective combinations was performed (represented by + above the bars).

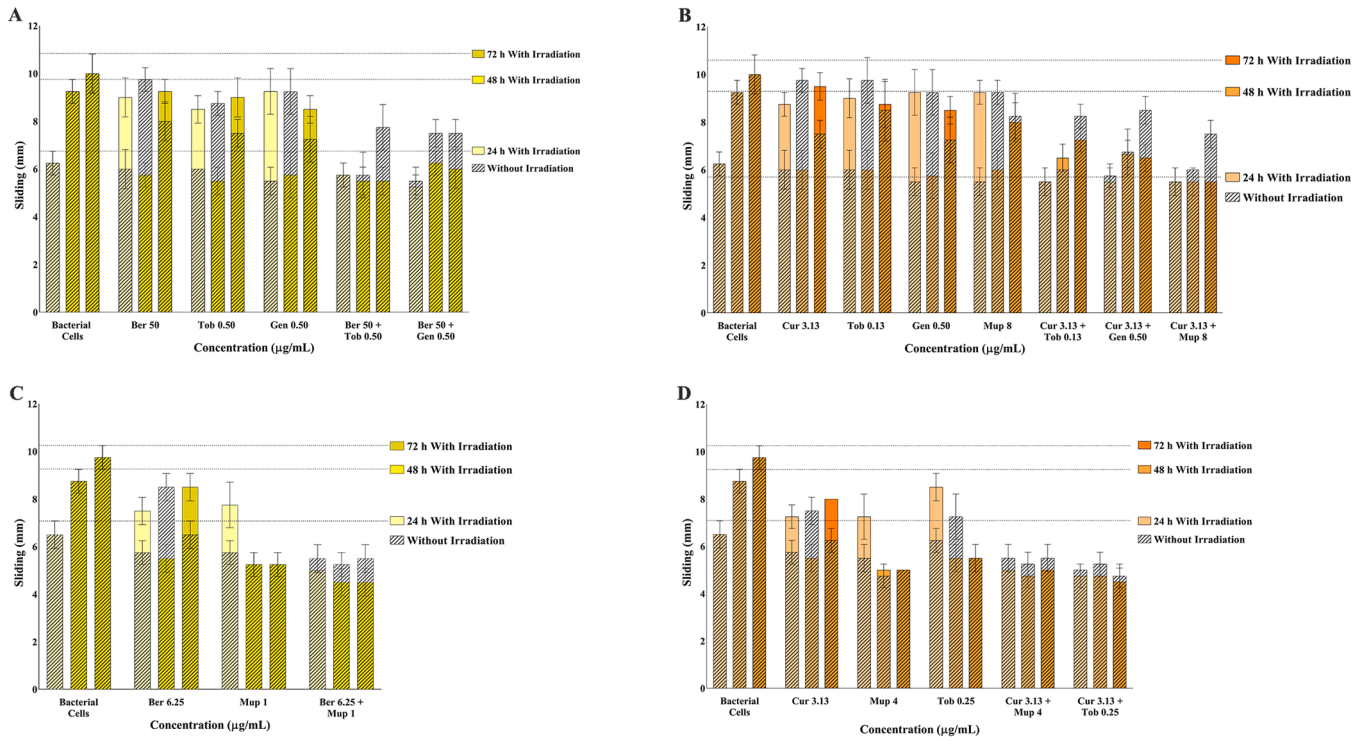

Fig. 7. Sliding motility (mm) over time of MRSA (A and B) and MSSA (C and D) strains after Ber-Ab (A and C) and Cur-Ab (B and D) combinations treatment at different concentrations, under irradiation and darkness conditions. Data are presented as mean ± SDs for two independent experiments with at least three replicates. Statistical analyses are presented in **Table S2**.

reducing Lip production in the MRSA strain (Fig. 8**E** and **F**). In particular, Ber-Tob, Cur-Gen (which had a synergistic effect (+++) compared to photoactivated Ber, Cur, Tob and Gen alone) and Cur-Mup (additive effect (++) compared with photoactivated Cur and Mup), while Mup alone led to a significant reduction ($P < 0.05$, **Table S4**).

4. Discussion

The emergence of antibiotic-resistant strains such as MRSA makes treating *S. aureus* wound infections even more difficult [40]. Bacteria have a distinct ability to adapt to high-stress situations [13]. Nevertheless, when simultaneously exposed to different stress stimuli, bacteria may not be able to develop different responses to cope with all stimuli [22]. This high stress pressure could be a promising solution to effectively overcome antibiotic resistance. In this sense, photoactivation of Ber-Ab and Cur-Ab combinations may represent an effective therapeutic multi-target strategy. Despite the various known modes of action of ROS, this study is pioneering in investigating the targets of blue light photoactivated and non-photoactivated Ber-Ab and Cur-Ab combinations. In addition, the 6 h incubation time of the combinations more accurately simulates a realistic topical application in the clinic, further emphasizing the novelty of this study. First, we studied the ability of the combined approach to generate ROS and then evaluated the effects of ROS and Ber-Ab and Cur-Ab combinations on membrane integrity, DNA damage, motility, and key virulence factors associated with the establishment of *S. aureus* acute skin wound infections. All these mechanisms were explored in both MSSA and MRSA strains to observe the influence of bacterial susceptibility profiles on the performance of the combined strategy.

In aPDI, the activation of PS through light absorption produces ROS, which are responsible for its therapeutic effect. The process occurs when an electron is stimulated from its ground state to an excited singlet state. After passing through the system, this excited state becomes a triplet state (^{3}PS), which has a comparatively long half-life. ROS are generated by the triplet state via two different photoprocesses (type I and II) [41]. In type I, an electron is transferred from the ^{3}PS to a substrate, which is often a biomolecule. This produces an intermediate that combines with molecular oxygen in the ground state ($^3O_2$) and generates a superoxide radical ($O_2^{\bullet-}$). After the Haber-Weiss reaction, this radical reacts further and forms other ROS, such as H_2O_2 and $OH^{\bullet}$. Type II is a triplet-to-triplet energy transfer between ^{3}PS and $^3O_2$, leading to the formation of a short-lived, highly cytotoxic molecular singlet oxygen (O_2*), whereas type I is a charge transfer [13]. ROS cause a high degree of bacterial cytotoxicity by promoting the destruction of the bacterial membrane. Moreover, ROS can cause damage by oxidizing intracellular biomolecules such as nucleic acids and proteins [42]. Although bacteria have defense mechanisms to neutralize low levels of ROS, excessive production of ROS can overwhelm these defense mechanisms and lead to oxidative stress and cell damage [43].

In the present study, it was possible to observe the production of ROS in all the conditions tested, even without irradiation. This effect is related to the inherent potential of tested phytochemicals and antibiotics tested to produce ROS. Ber and Cur have been identified as ROS producers even without photoactivation [14,23,24,44]. For example, Zhang et al. [23], demonstrated the production of ROS in a MRSA strain after treatment with Ber (at 128 µg/mL). Likewise, it was also reported that Cur (at 192 µg/mL) increased the ROS concentration in *Escherichia coli* [14].

Despite limited information on the mechanism by which Gen, Mup, and Tob increase oxidative stress, the observed results could be due to their chemical structure (Fig. 1). The antibiotics tested have a structure rich in hydroxyl groups (OH^-) and when an electron is removed from the OH configuration, the hydroxyl radical ($OH^{\bullet}$) is formed [45]. However, a significant decrease in ROS values was observed from Mup and Tob exposure and photoactivation. This effect could be due to the chemical changes induced by the irradiation of these compounds with blue light, which led to a decrease in the amount of OH^- and thus reduced their ability to increase ROS levels. These changes could be indirectly

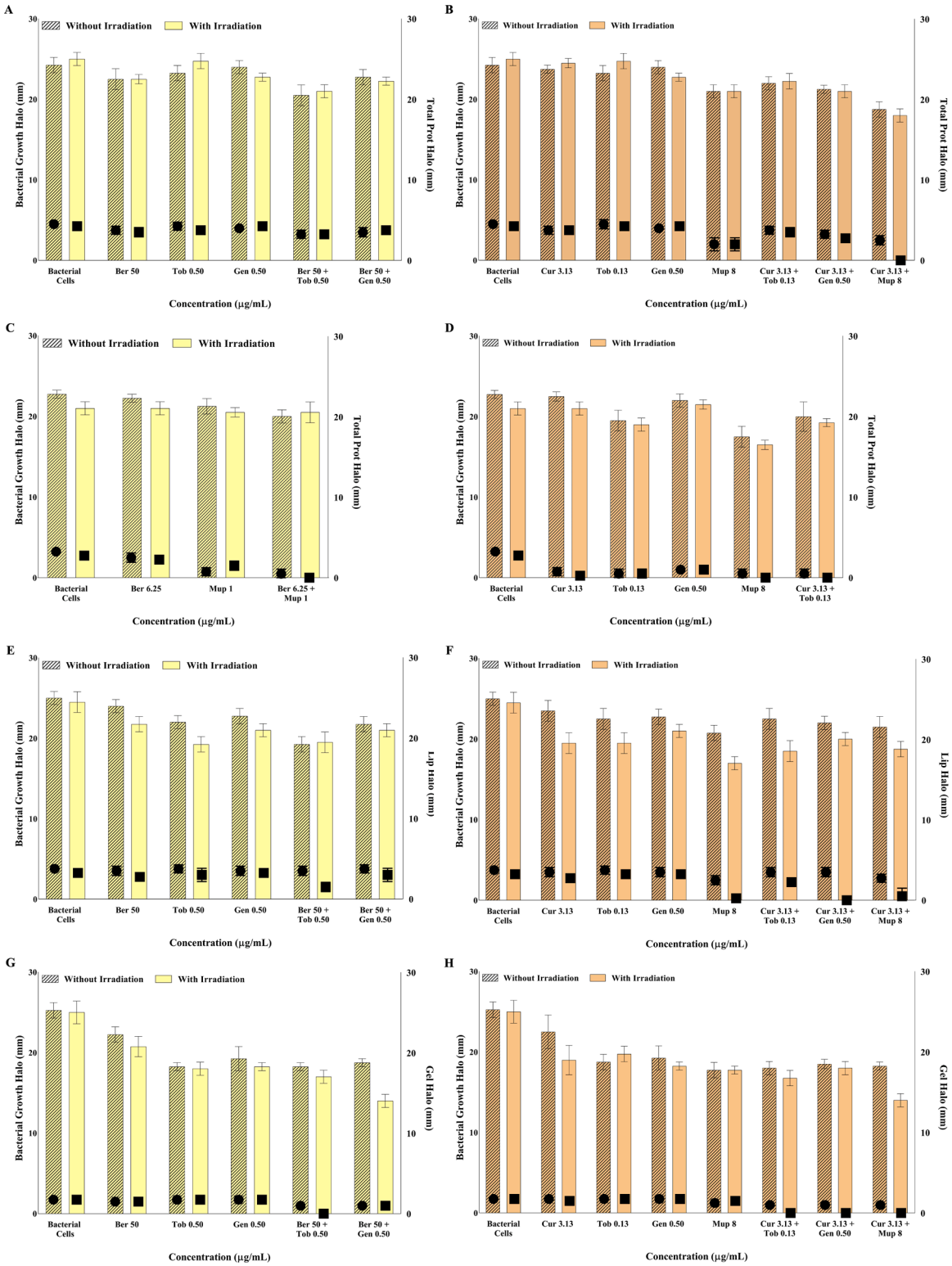

Fig. 8. Production of total Prot (A, B, C, and D), as well as Lip (E and F) and Gel (G and H) by MRSA (A, B, E, F, G, and H) and MSSA (C and D) strains after Ber-Ab (A, C, E, and G) and Cur-Ab (B, D, F, and, H) combinations treatment at different concentrations, under irradiation and darkness conditions. Data are presented as mean ± SDs for two independent experiments with at least three replicates. Statistical analyses were presented in **Table S3**.

promoted by the activation of bacterial enzymes responsible for chemical reactions that affect the structure of the antibiotic [45]. In contrast to these results, photoactivated Mup showed the opposite effect in MRSA and led to an increase in ROS levels. This could be due to increased oxidative stress, as an increase in ROS levels has been described as a possible bacterial response to stressful situations [46]. The observed decrease in ROS levels for Mup at 1 and 4 μg/mL after photoactivation in the MSSA strain, compared to the increase observed in the MSSA strain with Mup at 8 μg/mL, can be attributed to the different oxidative stress responses between these bacterial strains [47]. MRSA and MSSA strains have different regulatory pathways to cope with oxidative stress, which could explain the strain-specific responses to the photoactivated Mup

[46]. In MRSA, the lower concentration of Mup could trigger stronger bacterial defense mechanisms. This defense appears to lead to a reduction in ROS levels by scavenging ROS more effectively at lower antibiotic concentrations. On the other hand, the photoactivation of Mup at a higher concentration (8 μg/mL) in MSSA probably overwhelms the oxidative defense systems of bacteria, leading to an increase in ROS production.

Alongside the inherent ROS production capacity of each compound, exposure to blue light significantly increased this capacity, which is particularly noticeable after exposure to Ber-Ab and Cur-Ab combinations. The photoactivation of Ber and Cur has been reported to be associated with their increased phototoxicity [44,48]. However, a decrease in ROS production by MRSA after contact with photoactivated Ber was observed when compared to non-irradiated conditions. This effect can be attributed to the fact that Ber at the concentration tested (50 μg/mL) may not have the potential to cause a significant increase in ROS production when photoactivated. Moreover, it is crucial to highlight that ROS have a short lifetime [49]. Since ROS measurement occurred 6 h after photoactivation, it is important to recognize that the measured ROS amount may not precisely represent that generated during irradiation. The incubation time could help the bacteria to activate defense mechanisms against the ROS produced and reduce their levels [43].

In combination with the respective antibiotics, the duration of the antibacterial effect of Ber may be prolonged over time, which contradicts the immediate effect after photoactivation. In fact, phytochemicals and antibiotics used in combination could synergistically interact to disrupt bacterial homeostasis, enhancing ROS production [18]. Such effect could be corroborated by the lower efficacy of non-photoactivated combinations of Ber-Ab and Cur-Ab compared to the individual compounds. This phenomenon could be explained by possible interactions between the phytochemicals and the antibiotics [21]. In combination, these compounds might stabilize each other or result in a lower oxidative response from the bacteria, especially in the absence of photoactivation. The synergistic effects of these combinations are more pronounced when subjected to photoactivation, probably due to the activation of ROS-generating pathways specific to light exposure [17]. The lower ROS formation without light may also indicate that the full potential of the combination is only realized during the photodynamic process, further enhancing the antimicrobial activity upon photoactivation. In our recent study, the photodynamic potential of Ber-Ab and Cur-Ab combinations was investigated, where a remarkable efficacy was observed in inactivating both MRSA and MSSA strains [21]. Notably, a complete inhibition of culturability was verified after 6 h of incubation. These results corroborate the ROS production data obtained in the present study, where the photoactivated combinations originated higher ROS levels, resulting in the complete inactivation of both *S. aureus* strains. Although there is a clear correlation between ROS production and photodynamic antimicrobial activity, it is noteworthy that photoactivation with blue light was not the only contributor to ROS formation. Consequently, the interaction of antibiotics, phytochemicals, and blue light proved to be an effective strategy to achieve complete loss of culturability of *S. aureus* strains and at the same time increased ROS production.

ROS target the bacterial membrane and promote various effects that compromise its integrity [42]. Indeed, the photoactivation of Ber and Cur resulted in a higher reduction of the membrane integrity compared to non-photoactivated cells and the positive controls, which is consistent with the results of ROS production. These results are consistent with previous data [23,50,51]. For example, Jiang et al. [51], observed that Cur when activated by blue light induced stronger red fluorescence in *S. aureus* compared to untreated bacterial cells. In the present study, it is noteworthy that the percentage of cells stained with PI was higher with photoactivated Ber-Ab and Cur-Ab combinations than with Ber, Cur, and the antibiotics alone. However, in MSSA the non-photoactivated Ber-Ab and Cur-Ab combinations had a lower effect than the respective compounds alone, which is coherent with the results of ROS production, suggesting an antagonistic effect. In the case of Mup and Tob, photoactivation showed no significant effect except for Mup (at 1 μg/mL), where a slight decrease in the percentage of cells stained with PI was observed. These results are also consistent with the ROS results, where a decrease was observed for photoactivated Mup at 1 μg/mL.

The strong correlation between ROS production and PI uptake results confirms the key role of ROS as a disruptors of membrane integrity. ROS can attack and damage the lipid molecules that make up the bacterial cell membrane. This can occur through lipid peroxidation, where ROS react with the unsaturated fatty acids in the lipid bilayer and generate peroxides and other reactive products. These products can lead to degradation of membrane lipids, resulting in loss of cell membrane integrity and increased permeability [47]. ROS can also damage membrane proteins by oxidizing their amino acid residues, causing protein dysfunction. In this case, the membrane proteins are no longer able to fulfill their roles in maintaining membrane integrity and transport functions [52]. Furthermore, the results demonstrate that ROS production capacity is sustained even in the absence of photoactivation. This intrinsic ROS-generating ability is also evident in the capacity of non-photoactivated Ber-Ab and Cur-Ab to induce significant membrane damage.

Although the strong activity of ROS increased the membrane damage of both *S. aureus* strains, it is also possible to link this activity to the intrinsic antibacterial properties of Ber and Cur without photoactivation, as observed in the results of the positive controls used. Much is already known about the mode of action of Cur, particularly its effects on bacterial membranes [53]. The impairment of membrane integrity is related to its lipophilic structure, which allows it to penetrate deep into the membrane, disrupting 1,2-dipalmitoyl-sn-glycero-3-phosphocholine and interfering with exocytotic and membrane fusion processes [14,25]. On the other hand, Ber can increase the fluidity of membrane lipids and alter the conformation of membrane proteins [23].

Changes in membrane integrity lead to an imbalance of ions, including K^+, which is important for the regulation of cellular processes [54]. The results showed that all conditions tested, even without photoactivation, led to increased K^+ release by both strains. These results are also consistent with the PI uptake experiments, where an increase in membrane damage was observed for all the conditions without irradiation. These results follow other works that have studied the effect of phytochemicals without any irradiation [31,54]. For example, Borges et al. [54], observed that two phytochemicals, allylisothiocyanate and 2-phenylethylisothiocyanate, increased K^+ release in *S. aureus* CECT 976 (1.14 and 0.92 μg/mL, respectively, *versus* 0.78 of the control). Additionally, a strong correlation was observed between PI uptake and K^+ release, confirming the ion imbalance caused by membrane disruption.

The release of K^+ by MSSA was slightly higher than the values obtained for the MRSA strain without blue light irradiation. While our results differ slightly from those of Borges et al. [54], for the same *S. aureus* strain, it is important to note that a full correlation could not be established because our study used an incubation time of 6 h in NaCl, which does not provide the ideal conditions for normal bacterial growth and may lead to changes in membrane permeability and consequently to the release of K^+. Hajmeer et al. [55], for example, investigated the effect of NaCl on the cell morphology of *E. coli* (ATCC 51657, 43889, 35150, 43894, and 43895) and *S. aureus* strains (ATCC 13565, 25923, 27154, 27664 and 29213). For this purpose, different concentrations of NaCl (0 %, 5 %, and 10 %) were used, which were incorporated into the brain-heart infusion broth. The results showed that cell damage was dependent on the NaCl concentration. It was also found that *E. coli* strains showed lower tolerance to NaCl than *S. aureus* strains. The authors reported some changes in the membrane permeability of *S. aureus*. However, transmission electron microscopy images showed that the structural integrity of the membrane was maintained, indicating that the growth environment was still conducive to microbial proliferation. These results indicate that although NaCl slightly decreases membrane

permeability, the observed changes in membrane integrity do not affect the viability of *S. aureus*. Similar results were observed in our study for bacterial cells irradiated with blue light alone, which resulted in increased K^+ release in both strains. This differs from the results of the PI uptake recording, which showed no effect of blue light irradiation on bacterial membrane integrity. Dos Anjos et al. [56], for example, investigated the antibacterial effect of blue light alone against *S. aureus* (ATCC 25923), *E. coli* (ATCC 25922) and *Pseudomonas aeruginosa* (ATCC 27853). Different doses of blue light at 410 ± 10 nm (38.2 mW/cm^2) were used. The authors determined the lethal dose of blue light irradiation that killed 90 and 99.9 % of the three bacterial strains. The results showed that the two Gram-negative bacteria were more sensitive to the antibacterial effect of blue light irradiation than the *S. aureus* strain. The authors found that sublethal doses of blue light (< 63.5 J/cm^2) did not damage the cell membrane of *S. aureus*. The incorporation of PI was only detected after a blue light exposure of 549.6 J/cm^2, which was higher than the lethal dose that killed 100 % of the bacteria (397.7 J/cm^2). The light dose used in the present work (18 J/cm^2) was much lower than that used in the above-mentioned study [56]. The increase in K^+ level could be related to membrane permeability without obvious structural damage, such as activation of ion channels or changes in the conformation of membrane proteins [57]. Nevertheless, a strong correlation between K^+ release and PI uptake results was observed. For example, photoactivated Ber-Ab and Cur-Ab combinations led to increased K^+ release in the MRSA strain (≈ 90 %). In the case of the MSSA strain, membrane permeability to PI (approximately 40 %) did not appear to be related to the striking K^+ release when Ber-Ab and Cur-Ab were photoactivated. These results may confirm that the membrane of the MSSA strain is completely disrupted, which promotes the release of intercellular components such as K^+. For example, a significant decrease in the number of total cells treated with photoactivated Ber-Ab and Cur-Ab combinations was observed, mostly in comparison to those not photoactivated (Fig. 5). This decrease can be explained by the severe damage of bacterial cell membranes [58]. This phenomenon could affect PI staining and possibly lead to an underestimation of the proportion of bacterial cells with damaged membranes, as has been emphasised elsewhere [59]. Changes in membrane integrity could also promote modifications in the bacterial surface charge. Therefore, changes in surface charge that may occur due to membrane damage, affecting the adhesion properties of bacteria and their susceptibility to environmental stresses [60,61].

Both bacterial cells tested without treatment had a negative surface charge, which can be attributed to the presence of anionic groups (*e.g.* carboxyl and phosphate) [62]. However, the photoactivation of Ber-Ab and Cur-Ab combinations and the respective compounds alone leads to slight changes in the surface charge of the MRSA strain to less negative values. This increase in zeta potential to less negative values can be associated with a more permeable membrane [63]. Furthermore, there were no substantial changes between all conditions without blue light irradiation. The bacterial surface charge of the MSSA strain also did not change considerably under all non-photoactivated and photoactivated conditions. These results align with the findings of Borges et al. [54], who reported that some phytochemicals cause substantial damage to the *S. aureus* membrane but do not cause significant changes to the bacterial surface charge. Although the bacterial membrane damage may affect the surface charge, this study has shown that the present strategy does not effectively destabilize the bacterial surface charge. This fact could be due to the photoactivated Ber-Ab and Cur-Ab combinations being not able to induce changes in the structure or composition of the carboxyl and phosphate groups, which interferes with the bacterial surface charge [62].

Significant DNA damage was observed from the use of all Ber-Ab and Cur-Ab combinations and the respective compounds alone. Indeed, a strong correlation was observed between ROS production and DNA damage, underscoring the pivotal role of ROS in inducing DNA damage. Furthermore, the remarkable ability of all photoactivated Ber-Ab and Cur-Ab combinations to increase DNA damage is attributed to the amplified effect between the intrinsic DNA damage of all compounds tested and the ROS generated by photoactivated Ber-Ab and Cur-Ab combinations. These results are consistent with other studies, as all compounds tested can damage DNA, even without photoactivation [14, 64–67]. Ber can inhibit DNA synthesis, while Cur inhibits the bacterial DNA damage response (SOS response) and interacts with DNA molecules [14,15]. This genotoxic activity can be related to the upregulation of key proteins involved in DNA damage response and repair mechanisms. Karaosmanoglu et al. [68], found that the RecA protein in *E. coli* was significantly upregulated after Ber treatment. RecA is crucial for DNA repair and recombination, SOS response, horizontal gene transfer, motility, and biofilm formation. On the other hand, the aminoglycoside antibiotics Gen and Tob bind to bacterial ribosomes, interfering with the translation process and ultimately inhibiting the synthesis of bacterial proteins, which may indirectly lead to DNA damage in bacteria, resulting in the production of misfolded or partially folded proteins [69]. The accumulation of these abnormal proteins can overwhelm bacterial protein quality control systems and lead to the formation of protein aggregates [70], which can disrupt normal cellular processes and potentially contribute to DNA damage [71]. Similarly, Mup reversibly inhibits isoleucyl transfer RNA, thereby inhibiting bacterial protein and RNA synthesis [67]. These mechanisms can also increase the production of misfolded proteins and thereby cause DNA damage [71].

The DNA damage results obtained with PI and AO were generally consistent, confirming the effectiveness of both methods in detecting double-stranded DNA damage. Despite the same tendency of PI and AO results (which was also confirmed by ∑CI scoring), some results differed slightly. In fact, PI and AO bind to DNA in distinct ways, making them sensitive to different types of damage. PI intercalates between the bases of double-stranded DNA, particularly in regions where the helix exposes the bases, strongly binding to the DNA [59]. Its interaction with DNA is less selective regarding the conformation or structure of the molecule. Even if the DNA is damaged, by double-strand breaks or distortions, PI can still penetrate the damaged area and generate red fluorescence [72]. However, PI does not distinguish between specific types of DNA damage, such as small base changes or structural alterations that do not involve complete breaks [73]. In contrast, AO is more sensitive to structural changes in double-strand DNA, including minor distortions in the helix caused by subtle damage, such as oxidation or base modifications. When AO binds to double-strand DNA, it intercalates between the nitrogenous bases, mainly in purine-rich segments (adenine and guanine), producing intense green fluorescence [34]. AO binds to DNA more flexibly and specifically, and its green fluorescence is enhanced when it efficiently intercalates into the intact double helix. In addition, AO can also bind to single-strand DNA and RNA through distinct mechanisms. Its binding to single-strand DNA and RNA primarily occurs via electrostatic interactions with the negatively charged phosphate backbone or stacking interactions with unpaired bases [74]. Unlike its intercalation into double-stranded DNA, binding to single-strand DNA and RNA typically results in less stable associations and produces red fluorescence. This heightened sensitivity of AO to minor structural changes allows for more precise and comprehensive detection of DNA damage, including impairment that does not result in complete strand breaks but still impacts the conformation of the helix.

Motility plays a crucial role in the physiology of bacteria and influences vital functions such as colonization, biofilm formation, and the ability to adapt to different environments. Although *S. aureus* is a non-flagellated bacterium, it exhibits a particular form of motility known as sliding or colony spreading [75]. All combinations tested significantly reduced the motility of both strains after 24 h, but only the photoactivated combinations were able to maintain this reduction up to 72 h. The reduction observed may be due to oxidative stress caused by the intrinsic antibacterial activity of each compound used [64]. This assumption is confirmed by the effect of positive control - H_2O_2 at 3 % (v/v), which acts through the production of ROS. This oxidative stress condition could downregulate the activity of motility-related gene

expression and, consequently, help *S. aureus* to preserve resources and energy under pressure [76]. Additionally, the strong correlation observed between PI uptake, DNA damage, and sliding results highlights the significant impact of DNA damage and membrane disruption on bacterial motility. When combined, these effects compromise both the structural integrity and energy systems essential for bacterial motility [13].

The production of virulence factors plays a crucial role in the ability of bacteria to evade the host immune system, cause tissue damage, and establish persistent infections [77]. Actually, *S. aureus* can cause a wide range of infections due to its diverse virulence factors. These factors enable the bacterium to adhere to surfaces, invade the immune system, and exert toxic effects on the host [78]. Among the virulence factors with potential implications for skin wound infections are Prot, including Gel and Lip [79]. Prot plays a crucial role in delaying the wound healing process, thus increasing the likelihood of chronic wound infections [80]. However, it is worth noting that the majority of Prot found in non-healing wounds are produced by the host in response to the ongoing inflammation [80]. Lip is an important virulence factor produced by *S. aureus* during wound infections of the skin. These enzymes can weaken host granulocyte function and enhance bacterial survival during host defense by deactivating germicidal lipids [81]. When *S. aureus* colonizes the skin, it degrades human sebum by liphydrolysis and uses it as a nutrient source. This process not only maintains bacterial growth but also significantly reduces the skin's barrier function [82]. *S. aureus* has been reported to produce Gel, also known as type IV collagenase [83]. These enzymes act by specifically cleaving the collagen sequence in the extracellular matrix, thereby increasing the ability of the bacteria to infect the host [84]. It has been observed that *S. aureus* can trigger secondary activation of Gel in the host, contributing to the proteolytic activity necessary for dissemination in infected host tissue [85]. The production of Lip and Gel has been described for some *S. aureus* strains [82,83]. However, the strains differ from each other, which leads to variations in the production of virulence factors. The incubation time of 6 h in NaCl seems to influence the conformation of *S. aureus*. For example, in K^+ release results, higher values were observed for the MSSA strain compared to the MRSA strain. This altered performance of the MSSA strain could potentially affect normal Lip and Gel production [86]. In addition, the high antibiotic resistance of the MRSA strain could contribute to its increased tolerance in hostile environments, allowing it to exhibit a more virulent behavior [40].

Despite all these differences, photoactivation of Ber-Ab and Cur-Ab combinations showed great potential to enhance the anti-virulence activity of combinations without irradiation. In fact, Ber-Ab and Cur-Ab combinations led to increased ROS levels, membrane damage, K^+ release, DNA damage, and bacterial motility (Fig. 9). These effects not only impair the motility of *S. aureus* but also hinder its ability to express and secrete virulence factors, as evidenced by the reduced production of Total Prot, Gel, and Lip. The inhibition of Prot, which are crucial for the adhesion and degradation of host substrates, may be an indirect consequence of this damage. Oxidative stress and structural alterations resulting from membrane and DNA damage can impair the expression and activity of these enzymes, ultimately leading to a decrease in bacterial virulence. The oxidative stress promoted by photoactivation can disrupt regulatory pathways responsible for the production of total Prot, including Lip and Gel, leading to a decrease in the expression of these enzymes [22]. Hu et al. [26], found that Cur can effectively inhibit the activity of sortase A (belonging to the cysteine Prot family) in *Streptococcus mutans* UA159. Additionally, Cur has been reported to reduce important virulence factors such as alpha-hemolysin (Hla) and protein A (Spa), as well as the expression of the respective genes (*hla* and *spa*), indicating its ability to suppress the production of virulence factors [87,88].

Added to the observed remarkable multi-target effect of all Ber-Ab and Cur-Ab combinations, a critical consideration in the development of antimicrobial therapies for wound infections is the potential cytotoxicity of the compounds employed. For instance, the median lethal dose (LD50) values for Ber in rats following oral administration are reported to be 329 mg/kg [89]. Nonetheless, the concentrations of Ber utilized in the present study are significantly lower, indicating a

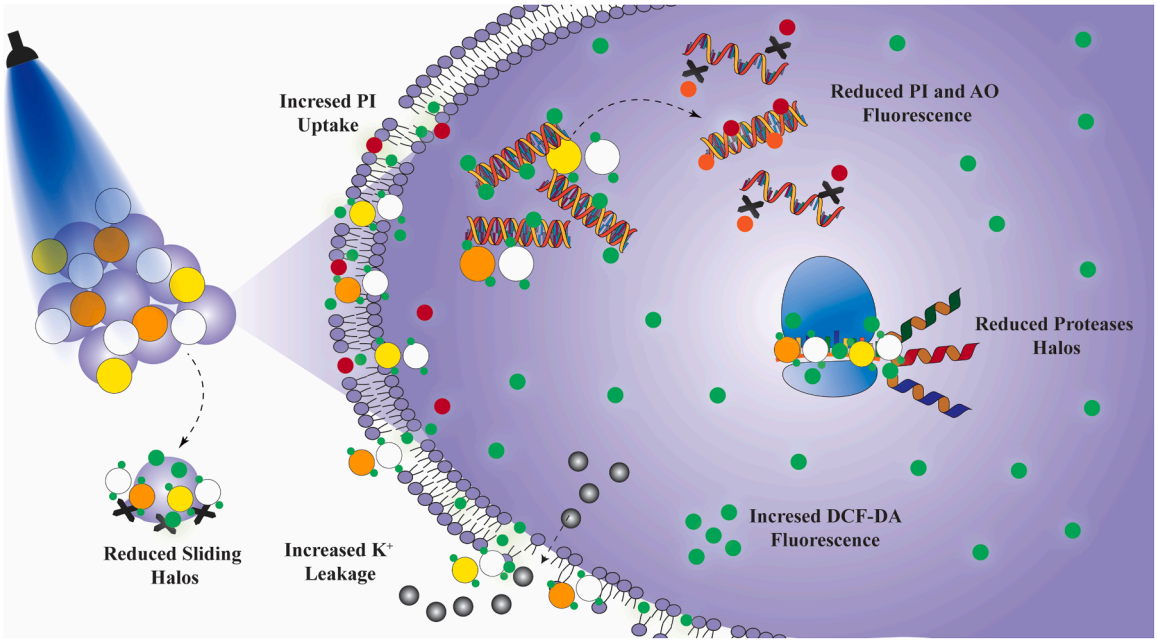

Fig. 9. Proposed antibacterial mode of action of blue light photoactivated Ber-Ab and Cur-Ab combinations against *S. aureus*. Upon photoactivation, these combinations triggered a marked increase in ROS production leading to severe oxidative stress. This process caused substantial damage to the bacterial cell membranes, with approximately 90 % disruption in MRSA and 40 % in MSSA, as evidenced by the significant release of intracellular K^+ (≈2.00 μg/mL in MRSA and 2.40 μg/mL in MSSA). Additionally, the treatment inflicted considerable DNA damage (≈ 50%) in both strains. Beyond its bactericidal effects, aPDI treatment also impaired *S. aureus* pathogenicity by reducing motility and inhibiting key virulence factors, including Prot, Lip and Gel, which are critical for infection progression. These results underscore the multi-target activity of Ber-Ab and Cur-Ab combinations in aPDI as a novel strategy to combat *S. aureus* infections effectively.

substantial margin of safety. Similarly, Cur has demonstrated no toxic effects even at high doses, with oral administration of up to 5000 mg/kg for 14 days showing no adverse reactions [90]. This remarkably low toxicity profile of curcumin underscores the safety of the Cur-Ab combinations in the present study, especially since the concentrations used were well below the tabulated value.

Concerning antibiotics, Mup topical ointments typically use a concentration of 2% (20 mg/mL) [91]. Similarly, Gen ointments and creams are commonly formulated at a concentration of 0.1% (1 mg/mL), while Tob eye ointments contain a concentration of 0.3% (3 mg/mL) [92,93]. It is noteworthy that the concentrations used in the present study are significantly lower than those employed in clinical settings, emphasizing the safety margin of our experimental approach. Additionally, it is important to recognize that the toxicity associated with topical applications may differ from oral administration due to variations in absorption, metabolism, and distribution. Topical administration often results in lower systemic exposure, thereby reducing the likelihood of systemic toxicity [28].

5. Conclusion

This study showed the multi-target activity of photoactivated and non-photoactivated Ber-Ab and Cur-Ab combinations. Blue light irradiation contributed significantly to increasing the action of all combinations tested. In particular, photoactivated Ber-Ab and Cur-Ab combinations were able to induce significant ROS production even at low concentrations. Although blue light irradiation notably augmented ROS production capacity, it is noteworthy that all compounds individually and without irradiation exhibited considerable ROS generation potential. The strong induction of ROS created an initial oxidative stress environment that leads to a remarkable decrease in membrane integrity, as confirmed by the release of K^+. Following this destabilization, all compounds interacted with the intracellular content, promoting effective antibacterial activity. The compounds further exhibited a remarkable potential to induce DNA damage, even without blue light irradiation. Photoactivated Ber-Ab and Cur-Ab combinations were able to reduce the virulence and pathogenicity of *S. aureus* strains by impairing motility and Prot production.

While blue light irradiation exhibited a high potential to enhance the activity of all phytochemical-Ab combinations, an amplified effect was observed for these combinations without irradiation when compared to the respective compounds alone. Notably, despite the considerable potential observed across all combinations tested, those incorporating Ber consistently outperformed others across all bacterial physiological indices of both strains. These results suggest that photoactivation of Ber-Ab and Cur-Ab combinations could be an effective strategy for the treatment of topical *S. aureus* wound infections. Moreover, due to its multi-target nature, this approach could efficiently overcome bacterial resistance to antibiotics and restore their efficacy. Added to this, the present study provides a solid basis for future research involving biofilms and chronic wound models (*in vitro* and *in vivo*). By focusing on planktonic cultures, this approach enables controlled research into the effects of Ber-Ab and Cur-Ab combinations and the influence of incubation time on their antimicrobial activity, which could support the development of translational therapies for topical infections.

Glossary

AO: Acridine Orange
aPDI: Antimicrobial photodynamic inactivation
Ber: Berberine
Ber-Ab: Berberine-antibiotic combinations
Cur: Curcumin
Cur-Ab: Curcumin-antibiotic combinations
dH_2O: Distilled water
DMSO: Dimethyl sulfoxide
EPS: Extracellular polymeric substances
Gel: Gelatinases
Gen: Gentamicin
DCF-DA-2′,7′: Dichlorodihydrofluorescein diacetate
K^+: Potassium
LBB: Luria-Bertani broth
LED: Light-emitting diode
Lip: Lipases
MHA: Mueller-Hinton agar
MHB: Mueller-Hinton broth
MIC: Minimum inhibitory concentration
MRSA: Methicillin-resistant *S. aureus*
MSSA: Methicillin-susceptible *S. aureus*
Mup: Mupirocin
NaCl: Sodium chloride
PCA: Plate count agar
PI: Propidium iodide
PS: Photosensitiser
Prot: Proteases
ROS: Reactive oxygen species
SDs: Standard deviations
Tob: Tobramycin

Data availability

Data will be made available on request.

CRediT authorship contribution statement

Ariana S.C. Gonçalves: Writing – original draft, Methodology, Investigation, Formal analysis, Conceptualization. **José R. Fernandes:** Writing – review & editing, Resources, Conceptualization. **Maria José Saavedra:** Writing – review & editing, Resources. **Nuno M. Guimarães:** Writing – review & editing, Methodology. **Cristiana Pereira:** Writing – review & editing, Supervision. **Manuel Simões:** Writing – review & editing, Supervision, Resources, Funding acquisition, Conceptualization. **Anabela Borges:** Writing – review & editing, Supervision, Resources, Project administration, Methodology, Conceptualization.

Declaration of competing interest

The authors declare that they have no known competing financial interests or personal relationships that could have appeared to influence the work reported in this paper.

Acknowledgments

This work was supported by the Project InnovAntiBiofilm (ref. 101157363) financed by European Commission (Horizon-Widera 2023-Acess-02/Horizon-CSA) and national funds through FCT/MCTES (PIDDAC): LEPABE, UIDB/00511/2020 (DOI: 10.54499/UIDB/00511/2020) and UIDP/00511/2020 (DOI:10.54499/UIDP/00511/2020) and ALiCE, LA/P/0045/2020 (DOI: 10.54499/LA/P/0045/2020). Ariana S. C. Gonçalves acknowledges individual PhD fellowships from FCT (2022.10913.BD).

Supplementary materials

Supplementary material associated with this article can be found, in the online version, at doi:10.1016/j.pdpdt.2025.104514.

References

[1] J. Hurlow, P.G. Bowler, Acute and chronic wound infections: microbiological, immunological, clinical and therapeutic distinctions, J. Wound Care 31 (5) (2022) 436–445.

[2] A. Borges, M.J. Saavedra, M. Simoes, Insights on antimicrobial resistance, biofilms and the use of phytochemicals as new antimicrobial agents, Curr. Med. Chem. 22 (21) (2015) 2590–2614.

[3] M.S. Almuhayawi, M.H. Alruhaili, H.S. Gattan, M.T. Alharbi, M. Nagshabandi, S. Al Jaouni, S. Selim, A. Alanazi, Y. Alruwaili, O.A. Faried, *Staphylococcus aureus* induced wound infections which antimicrobial resistance, methicillin-and vancomycin-resistant: assessment of emergence and cross sectional study, Infect. Drug Resist. 16 (2023) 5335–5346.

[4] Y. Zhang, Y. Zhu, A. Gupta, Y. Huang, C.K. Murray, M.S. Vrahas, M.E. Sherwood, D. G. Baer, M.R. Hamblin, T. Dai, Antimicrobial blue light therapy for multidrug-resistant *Acinetobacter baumannii* infection in a mouse burn model: implications for prophylaxis and treatment of combat-related wound infections, J. Infect. Dis. 209 (12) (2014) 1963–1971.

[5] A.C. Abreu, S.C. Serra, A. Borges, M.J. Saavedra, A.J. Mcbain, A.J. Salgado, M. Simoes, Combinatorial activity of flavonoids with antibiotics against drug-resistant *Staphylococcus aureus*, Microb. Drug Resist. 21 (6) (2015) 600–609.

[6] D. Oliveira, A. Borges, M.J. Saavedra, F. Borges, M. Simões, Screening of natural molecules as adjuvants to topical antibiotics to treat *Staphylococcus aureus* from diabetic foot ulcer infections, Antibiotics 11 (5) (2022) 620.

[7] S.P. Songca, Y. Adjei, Applications of antimicrobial photodynamic therapy against bacterial biofilms, Int. J. Mol. Sci. 23 (6) (2022) 3209.

[8] E. Polat, K. Kang, Natural photosensitizers in antimicrobial photodynamic therapy, Biomedicines 9 (6) (2021) 584.

[9] X. Shen, L. Dong, X. He, C. Zhao, W. Zhang, X. Li, Y. Lu, Treatment of infected wounds with methylene blue photodynamic therapy: an effective and safe treatment method, Photodiagnosis. Photodyn. Ther. 32 (2020) 102051.

[10] C. Opländer, S. Hidding, F.B. Werners, M. Born, N. Pallua, C.V. Suschek, Effects of blue light irradiation on human dermal fibroblasts, J. Photochem. Photobiol. B Biol. 103 (2) (2011) 118–125.

[11] L.P. Rosa, F.C. da Silva, S.A. Nader, G.A. Meira, M.S. Viana, Antimicrobial photodynamic inactivation of *Staphylococcus aureus* biofilms in bone specimens using methylene blue, toluidine blue ortho and malachite green: an *in vitro* study, Arch. Oral Biol. 60 (5) (2015) 675–680.

[12] S.M. Safai, K. Khorsandi, S. Falsafi, Effect of berberine and blue LED irradiation on combating biofilm of *Pseudomonas aeruginosa* and Staphylococcus aureus, Curr. Microbiol. 79 (12) (2022) 366.

[13] A.S. Gonçalves, M.M. Leitão, M. Simões, A. Borges, The action of phytochemicals in biofilm control, Nat. Prod. Rep. 40 (2023) 595–627.

[14] D. Zheng, C. Huang, H. Huang, Y. Zhao, M.R.U. Khan, H. Zhao, L. Huang, Antibacterial mechanism of curcumin: a review, Chem. Biodivers. 17 (8) (2020) e2000171.

[15] L. Peng, S. Kang, Z. Yin, R. Jia, X. Song, L. Li, Z. Li, Y. Zou, X. Liang, L. Li, C. He, G. Ye, L. Yin, F. Shi, C. Lv, B. Jing, Antibacterial activity and mechanism of berberine against *Streptococcus agalactiae*, Int. J. Clin. Exp. Pathol. 8 (5) (2015) 5217–5223.

[16] T.M. Branco, N.C. Valério, V.I.R. Jesus, C.J. Dias, M.G.P.M.S. Neves, M.A. F. Faustino, A. Almeida, Single and combined effects of photodynamic therapy and antibiotics to inactivate *Staphylococcus aureus* on skin, Photodiagnosis. Photodyn. Ther. 21 (2018) 285–293.

[17] F.-J. Schmitt, G. Renger, T. Friedrich, V.D. Kreslavski, S.K. Zharmukhamedov, D. A. Los, V.V. Kuznetsov, S.I. Allakhverdiev, Reactive oxygen species: *re*-evaluation of generation, monitoring and role in stress-signaling in phototrophic organisms, Biochim. Biophys. Acta (BBA) - Bioenerg. 1837 (6) (2014) 835–848.

[18] Y. Feng, C.C. Tonon, S. Ashraf, T. Hasan, Photodynamic and antibiotic therapy in combination against bacterial infections: efficacy, determinants, mechanisms, and future perspectives, Adv. Drug Deliv. Rev. 177 (2021) 113941.

[19] I.B. Gosbell, Methicillin-resistant *Staphylococcus aureus*: impact on dermatology practice, Am. J. Clin. Dermatol. 5 (2004) 239–259.

[20] A.F. Silva, A. Borges, C.F. Freitas, N. Hioka, J.M.G. Mikcha, M. Simões, Antimicrobial photodynamic inactivation mediated by rose Bengal and erythrosine is effective in the control of food-related bacteria in planktonic and biofilm states, Molecules 23 (9) (2018) 2288.

[21] A.S. Gonçalves, M.M. Leitão, J.R. Fernandes, M.J. Saavedra, C. Pereira, M. Simões, A. Borges, Photodynamic activation of phytochemical-antibiotic combinations for combatting *Staphylococcus aureus* from acute wound infections, J. Photochem. Photobiol. B Biol. 258 (2024) 112978.

[22] A.F. Seixas, A.P. Quendera, J.P. Sousa, A.F.Q. Silva, C.M. Arraiano, J.M. Andrade, Bacterial response to oxidative stress and RNA oxidation, Front. Genet. 12 (2022) 821535.

[23] X. Zhang, X. Sun, J. Wu, Y. Wu, Y. Wang, X. Hu, X. Wang, Berberine damages the cell surface of methicillin-resistant *Staphylococcus aureus*, Front. Microbiol. 11 (2020) 621.

[24] G.-F. Du, Y.-J. Le, X. Sun, X.-Y. Yang, Q.-Y. He, Proteomic investigation into the action mechanism of berberine against *Streptococcus pyogenes*, J. Proteomics 215 (2020) 103666.

[25] M. Duda, K. Cygan, A. Wisniewska-Becker, Effects of curcumin on lipid membranes: an EPR spin-label study, Cell Biochem. Biophys. 78 (2) (2020) 139–147.

[26] P. Hu, P. Huang, W.M. Chen, Curcumin inhibits the Sortase A activity of the *Streptococcus mutans* UA159, Appl. Biochem. Biotechnol. 171 (2) (2013) 396–402.

[27] S. Jaberi, F. Fallah, A. Hashemi, A.M. Karimi, L. Azimi, Inhibitory effects of curcumin on the expression of NorA efflux pump and reduce antibiotic resistance in *Staphylococcus aureus*, J. Pure Appl. Microbiol. 12 (1) (2018) 95–102.

[28] R.H. Demling, L. DeSanti, Management of partial thickness facial burns (comparison of topical antibiotics and bio-engineered skin substitutes) Supported in part by the heather foundation, Burns 25 (3) (1999) 256–261.

[29] J. Zhang, P. Zheng, J. Li, Y. Yang, S. Zeng, J. Qiu, S. Lin, Curcumin-mediated sono-photodynamic treatment inactivates listeria monocytogenes via ROS-induced physical disruption and oxidative damage, Foods 11 (6) (2022) 808.

[30] C. Ortega-Villasante, S. Burén, A. Blázquez-Castro, Á. Barón-Sola, L.E. Hernández, Fluorescent *in vivo* imaging of reactive oxygen species and redox potential in plants, Free Radic. Biol. Med. 122 (2018) 202–220.

[31] A. Borges, C. Ferreira, M.J. Saavedra, M. Simões, Antibacterial activity and mode of action of ferulic and gallic acids against pathogenic bacteria, Microb. Drug Resist. 19 (4) (2013) 256–265.

[32] Y. Gao, B. Mai, A. Wang, M. Li, X. Wang, K. Zhang, Q. Liu, S. Wei, P. Wang, Antimicrobial properties of a new type of photosensitizer derived from phthalocyanine against planktonic and biofilm forms of *Staphylococcus aureus*, Photodiagnosis. Photodyn. Ther. 21 (2018) 316–326.

[33] J.P. Diaper, C. Edwards, Survival of *Staphylococcus aureus* in lakewater monitored by flow cytometry, Microbiology (N Y) 140 (1) (1994) 35–42.

[34] N. Kure, T. Sano, S. Harada, T. Yasunaga, Kinetics of the interaction between DNA and acridine orange, Bull. Chem. Soc. Jpn. 61 (3) (1988) 643–653.

[35] A. Borges, L.C. Simões, M.J. Saavedra, M. Simões, The action of selected isothiocyanates on bacterial biofilm prevention and control, Int. Biodeterior. Biodegrad. 86 (2014) 25–33.

[36] A. Abdelmoteleb, R. Troncoso-Rojas, T. Gonzalez-Soto, D. González-Mendoza, Antifungical activity of autochthonous *Bacillus subtilis* isolated from Prosopis juliflora against phytopathogenic fungi, Mycobiology 45 (4) (2017) 385–391.

[37] M.A. Meheissen, M. Morsi, M. Hamad, M. Raouf, A one year single-center experience on *Stenotrophomonas maltophilia* strains in Alexandria, Egypt, Egypt J. Med. Microbiol. 31 (2) (2022) 69–76.

[38] M.d.F.S. Lopes, A.P. Simões, R. Tenreiro, J.J.F. Marques, M.T.B. Crespo, Activity and expression of a virulence factor, gelatinase, in dairy enterococci, Int. J. Food Microbiol. 112 (3) (2006) 208–214.

[39] J. Baptista, M. Simões, A. Borges, Effect of plant-based catecholic molecules on the prevention and eradication of *Escherichia coli* biofilms: a structure activity relationship study, Int. Biodeterior. Biodegrad. 141 (2019) 101–113.

[40] A.M. Algammal, H.F. Hetta, A. Elkelish, D.H.H. Alkhalifah, W.N. Hozzein, G. E. Batiha, N. El Nahhas, M.A. Mabrok, Methicillin-resistant *Staphylococcus aureus* (MRSA): one health perspective approach to the bacterium epidemiology, virulence factors, antibiotic-resistance, and zoonotic impact, Infect. Drug Resist. 13 (2020) 3255–3265.

[41] S. Rajesh, E. Koshi, K. Philip, A. Mohan, Antimicrobial photodynamic therapy: an overview, J. Indian Soc. Periodontol. 15 (4) (2011) 323.

[42] C.A. Juan, J.M. Pérez de la Lastra, F.J. Plou, E. Pérez-Lebeña, The chemistry of reactive oxygen species (ROS) revisited: outlining their role in biological macromolecules (DNA, lipids and proteins) and induced pathologies, Int. J. Mol. Sci. 22 (9) (2021) 4642.

[43] A. Vaishampayan, E. Grohmann, Antimicrobials functioning through ROS-mediated mechanisms: current insights, Microorganisms 10 (1) (2022) 61.

[44] C. Dai, J. Lin, H. Li, Z. Shen, Y. Wang, T. Velkov, J. Shen, The natural product curcumin as an antibacterial agent: current achievements and problems, Antioxidants 11 (3) (2022) 459.

[45] F. Xu, S. Cao, L. Shi, W. Chen, X. Su, Z. Yang, Blue light irradiation affects anthocyanin content and enzyme activities involved in postharvest strawberry fruit, J. Agric. Food Chem. 62 (20) (2014) 4778–4783.

[46] A. Rose, R. Shteynberg, M. Dasilva, J. Mixon, K. Mucciarone, L. Vu, K. Arsenault, V. Briand, S. Parker, S. Smith, C. Vise, C. Pina, L. Laranjo, Oxidative stress response in bacteria: a review, Fine Focus 8 (1) (2022) 36–46.

[47] M. Fasnacht, N. Polacek, Oxidative stress in bacteria and the central dogma of molecular biology, Front. Mol. Biosci. 8 (2021) 671037.

[48] C. Marques, M.H. Fernandes, S.A.C. Lima, Elucidating berberine's therapeutic and photosensitizer potential through nanomedicine tools, Pharmaceutics 15 (9) (2023) 2282.

[49] L.A. Del Río, ROS and RNS in plant physiology: an overview, J. Exp. Bot. 66 (10) (2015) 2827–2837.

[50] Y. Yuan, Q. Liu, Y. Huang, M. Qi, H. Yan, W. Li, H. Zhuang, Antibacterial efficacy and mechanisms of curcumin-based photodynamic treatment against *Staphylococcus aureus* and its application in juices, Molecules 27 (20) (2022) 7136.

[51] S. Jiang, R. Zhu, X. He, J. Wang, M. Wang, Y. Qian, S. Wang, Enhanced photocytotoxicity of curcumin delivered by solid lipid nanoparticles, Int. J. Nanomed. 12 (null) (2017) 167–178.

[52] Q. Xiang, Y. Wang, W. Wu, X. Meng, Y. Qiao, L. Xu, X. Liu, Carnosic acid protects against ROS/RNS-induced protein damage and upregulates HO-1 expression in RAW264. 7 macrophages, J. Funct. Foods 5 (1) (2013) 362–369.

[53] P. Tyagi, M. Singh, H. Kumari, A. Kumari, K. Mukhopadhyay, Bactericidal activity of curcumin I is associated with damaging of bacterial membrane, PLoS One 10 (3) (2015) e0121313.

[54] A. Borges, A.C. Abreu, C. Ferreira, M.J. Saavedra, L.C. Simões, M. Simões, Antibacterial activity and mode of action of selected glucosinolate hydrolysis products against bacterial pathogens, J. Food Sci. Technol. 52 (2015) 4737–4748.

[55] M. Hajmeer, E. Ceylan, J.L. Marsden, D.Y. Fung, Impact of sodium chloride on Escherichia coli O157: H7 and *Staphylococcus aureus* analysed using transmission electron microscopy, Food Microbiol. 23 (5) (2006) 446–452.

[56] C. Dos Anjos, L.G. Leanse, M.S. Ribeiro, F.P. Sellera, M. Dropa, V.E. Arana-Chavez, N. Lincopan, M.S. Baptista, F.C. Pogliani, T. Dai, New insights into the bacterial targets of antimicrobial blue light, Microbiol. Spectr. 11 (2) (2023) e02833. -22.

[57] A.V. Shubin, I.V. Demidyuk, A.A. Komissarov, L.M. Rafieva, S.V. Kostrov, Cytoplasmic vacuolization in cell death and survival, Oncotarget 7 (34) (2016) 55863–55889.

[58] T. Wang, M. Libardo, A. Angeles-Boza, J. Pellois, Membrane oxidation in cell delivery and cell killing applications, ACS Chem. Biol. (2017) 1170–1182.
[59] M. Rosenberg, N.F. Azevedo, A. Ivask, Propidium iodide staining underestimates viability of adherent bacterial cells, Sci. Rep. 9 (1) (2019) 6483.
[60] I. Barák, K. Muchová, The role of lipid domains in bacterial cell processes, Int. J. Mol. Sci. 14 (2) (2013) 4050–4065.
[61] S. Murínová, K. Dercová, Response mechanisms of bacterial degraders to environmental contaminants on the level of cell walls and cytoplasmic membrane, Int. J. Microbiol. 2014 (2014) 873081.
[62] J. Palmer, S. Flint, J. Brooks, Bacterial cell attachment, the beginning of a biofilm, J. Ind. Microbiol. Biotechnol. 34 (9) (2007) 577–588.
[63] S. Halder, K.K. Yadav, R. Sarkar, S. Mukherjee, P. Saha, S. Haldar, S. Karmakar, T. Sen, Alteration of zeta potential and membrane permeability in bacteria: a study with cationic agents, Springerplus 4 (1) (2015) 1–14.
[64] Z. Baharoglu, E. Krin, D. Mazel, RpoS plays a central role in the SOS induction by sub-lethal aminoglycoside concentrations in *Vibrio cholerae*, PLoS Genet. 9 (4) (2013) e1003421.
[65] J.M. Boberek, J. Stach, L. Good, Genetic evidence for inhibition of bacterial division protein ftsz by berberine, PLoS One 5 (10) (2010) e13745.
[66] R.S. Clarke, K.P. Ha, A.M. Edwards, RexAB promotes the survival of *Staphylococcus aureus* exposed to multiple classes of antibiotics, Antimicrob. Agents Chemother. 65 (10) (2021).
[67] S. Reiß, J. Pané-Farré, S. Fuchs, P. François, M. Liebeke, J. Schrenzel, U. Lindequist, M. Lalk, C. Wolz, M. Hecker, S. Engelmann, Global analysis of the *Staphylococcus aureus* response to mupirocin, Antimicrob. Agents Chemother. 56 (2) (2012) 787–804.
[68] K. Karaosmanoglu, N.A. Sayar, I.A. Kurnaz, B.S. Akbulut, Assessment of berberine as a multi-target antimicrobial: a multi-omics study for drug discovery and repositioning, Omics J. Integr. Biol. 18 (1) (2014) 42–53.
[69] K.M. Krause, A.W. Serio, T.R. Kane, L.E. Connolly, Aminoglycosides: an overview, Cold Spring Harb. Perspect. Med. 6 (6) (2016).
[70] L. Goltermann, M.V. Sarusie, T. Bentin, Chaperonin GroEL/GroES over-expression promotes aminoglycoside resistance and reduces drug susceptibilities in *Escherichia coli* following exposure to sublethal aminoglycoside doses, Front. Microbiol. 6 (2016) 1572.
[71] A. Mogk, D. Huber, B. Bukau, Integrating protein homeostasis strategies in prokaryotes, Cold Spring Harb. Perspect. Biol. 3 (4) (2011).
[72] W.D. Wilson, C. Krishnamoorthy, Y.H. Wang, J. Smith, Mechanism of intercalation: ion effects on the equilibrium and kinetic constants for the interaction of propidium and ethidium with DNA, Biopolym. Orig. Res. Biomol. 24 (10) (1985) 1941–1961.
[73] P.L. Olive, J.P. Banáth, The comet assay: a method to measure DNA damage in individual cells, Nat. Protoc. 1 (1) (2006) 23–29.
[74] D. Freifelder, P.F. Davison, E.P. Geiduschek, Damage by visible light to the acridine orange-DNA complex, Biophys. J. 1 (5) (1961) 389–400.
[75] J. Monte, A.C. Abreu, A. Borges, L.C. Simões, M. Simões, Antimicrobial activity of selected phytochemicals against Escherichia coli and *Staphylococcus aureus* and their biofilms, Pathogens 3 (2) (2014) 473–498.
[76] A. Jousselin, W.L. Kelley, C. Barras, D.P. Lew, A. Renzoni, The *Staphylococcus aureus* thiol/oxidative stress global regulator Spx controls trfA, a gene implicated in cell wall antibiotic resistance, Antimicrob. Agents Chemother. 57 (7) (2013) 3283–3292.
[77] A. Clinton, T. Carter, Biofilms and wounds: an overview of the evidence, Adv. Wound Care (New Rochelle) 4 (7) (2015) 373–381.
[78] D. Oliveira, A. Borges, M. Simões, *Staphylococcus aureus* toxins and their molecular activity in infectious diseases, Toxins (Basel) 10 (6) (2018) 252.
[79] M. Preda, M.M. Mihai, L.I. Popa, L.-M. Dițu, A.M. Holban, L.S.C. Manolescu, G.-L. Popa, A.-A. Muntean, I. Gheorghe, C.M. Chifiriuc, M.-I. Popa, Phenotypic and genotypic virulence features of staphylococcal strains isolated from difficult-to-treat skin and soft tissue infections, PLoS One 16 (2) (2021) e0246478.
[80] S.M. McCarty, S.L. Percival, Proteases and delayed wound healing, Adv. Wound Care (New Rochelle) 2 (8) (2013) 438–447.
[81] M. Park, E. Do, W.H. Jung, Lipolytic enzymes involved in the virulence of human pathogenic fungi, Mycobiology 41 (2) (2013) 67–72.
[82] M. Tanaka, S. Kamitani, K. Kitadokoro, *Staphylococcus aureus* lipase: purification, kinetic characterization, crystallization and crystallographic study, Acta Crystallogr. 74 (9) (2018) 567–570.
[83] S.P. Chakraborty, S.K. Mahapatra, S. Roy, Biochemical characters and antibiotic susceptibility of *Staphylococcus aureus* isolates, Asian Pac. J. Trop. Biomed. 1 (3) (2011) 212–216.
[84] L. Qiu, C. Wang, X. Lei, X. Du, Q. Guo, S. Zhou, P. Cui, T. Hong, P. Jiang, J. Wang, Y.Q. Li, J. Xia, Gelatinase-responsive release of an antibacterial photodynamic peptide against *Staphylococcus aureus*, Biomater. Sci. 9 (9) (2021) 3433–3444.
[85] M. Peetermans, T. Vanassche, L. Liesenborghs, J. Claes, G. Vande Velde, J. Kwiecinksi, T. Jin, B. De Geest, M.F. Hoylaerts, R.H. Lijnen, P. Verhamme, Plasminogen activation by staphylokinase enhances local spreading of *S. aureus* in skin infections, BMC Microbiol. 14 (2014) 310.
[86] L. Tuchscherr, B. Löffler, R.A. Proctor, Persistence of *Staphylococcus aureus*: multiple metabolic pathways impact the expression of virulence factors in small-colony variants (scvs), Front. Microbiol. 11 (2020) 1028.
[87] Y. Oogai, M. Matsuo, M. Hashimoto, F. Kato, M. Sugai, H. Komatsuzawa, Expression of virulence factors by *Staphylococcus aureus* grown in serum, Appl. Environ. Microbiol. 77 (22) (2011) 8097–8105.
[88] K. Arunachalam, P. Pandurangan, C. Shi, R. Lagoa, Regulation of *Staphylococcus aureus* virulence and application of nanotherapeutics to eradicate S. aureus infection, Pharmaceutics 15 (2) (2023) 310.
[89] M.M. Kheir, Y. Wang, L. Hua, J. Hu, L. Li, F. Lei, L. Du, Acute toxicity of berberine and its correlation with the blood concentration in mice, Food Chem. Toxicol. 48 (4) (2010) 1105–1110.
[90] V. Soleimani, A. Sahebkar, H. Hosseinzadeh, Turmeric (Curcuma longa) and its major constituent (curcumin) as nontoxic and safe substances, Phytother. Res. 32 (6) (2018) 985–995.
[91] A. Gangwar, P. Kumar, R. Singh, P. Kush, Recent advances in mupirocin delivery strategies for the treatment of bacterial skin and soft tissue infection, Future Pharmacol. 1 (1) (2021) 80–103.
[92] J. Cooley, N. Obaidi, V. Diaz, K. Anselmo, E. Eriksson, A.H. Carlsson, R.K. Chan, K. Nuutila, Delivery of topical gentamicin cream via platform wound device to reduce wound infection—A prospective, controlled, randomised, clinical study, Int. Wound J. 20 (5) (2023) 1426–1435.
[93] J.J. Dajcs, J.M. Moreau, D.W. Stroman, B. Schlech, T. Ke, B.A. Thibodeaux, D. O. Girgis, A.R. Caballero, R.J. O'Callaghan, The effectiveness of tobramycin and Ocuflox® in a prophylaxis model of *Staphylococcus keratitis*, Curr. Eye Res. 23 (1) (2001) 60–63.